AD-A126 155 THE DRAG OF A CIRCULAR CYLINDER ON OR NEAR A FLAT PLATE APPROPRIATE FOR S..(U) DAVID W TAYLOR NAVAL SHIP RESEARCH AND DEVELOPMENT CENTER BET.. C SUNG ET AL. 1/1

UNCLASSIFIED FEB 83 DTNSRDC/SPD-1018-01 F/G 20/4 NL

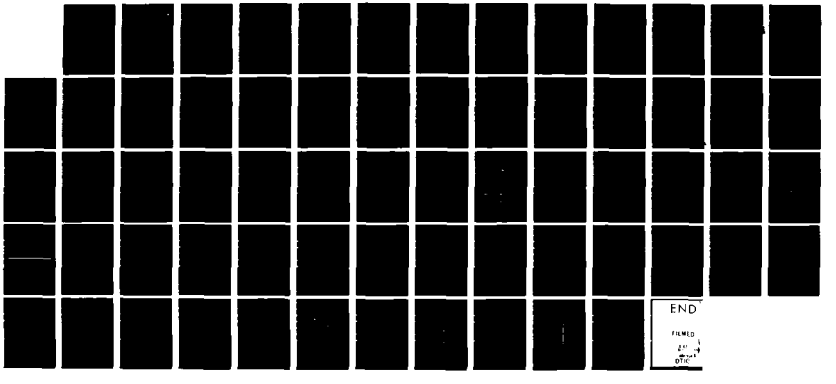

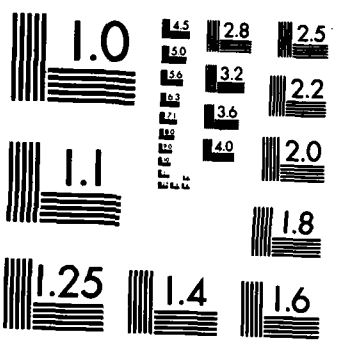

(12)

DAVID W. TAYLOR NAVAL SHIP RESEARCH AND DEVELOPMENT CENTER

Bethesda, Maryland 20084

DTNSRDC/SPD-1018-01

AD A126155

THE DRAG OF A CIRCULAR CYLINDER ON OR NEAR A FLAT PLATE APPROPRIATE FOR SHIP-MODEL TURBULENCE STIMULATORS

Chao-Ho Sung

and

Douglas S. Jenkins

APPROVED FOR PUBLIC RELEASE: DISTRIBUTION UNLIMITED

SHIP PERFORMANCE DEPARTMENT
DEPARTMENTAL REPORT

FEBRUARY 1983

DTNSRDC/SPD-1018-01

THE DRAG OF A CIRCULAR CYLINDER ON OR NEAR A FLAT PLATE APPROPRIATE FOR SHIP-MODEL TURBULENCE STIMULATORS

MAJOR DTNSRDC ORGANIZATIONAL COMPONENTS

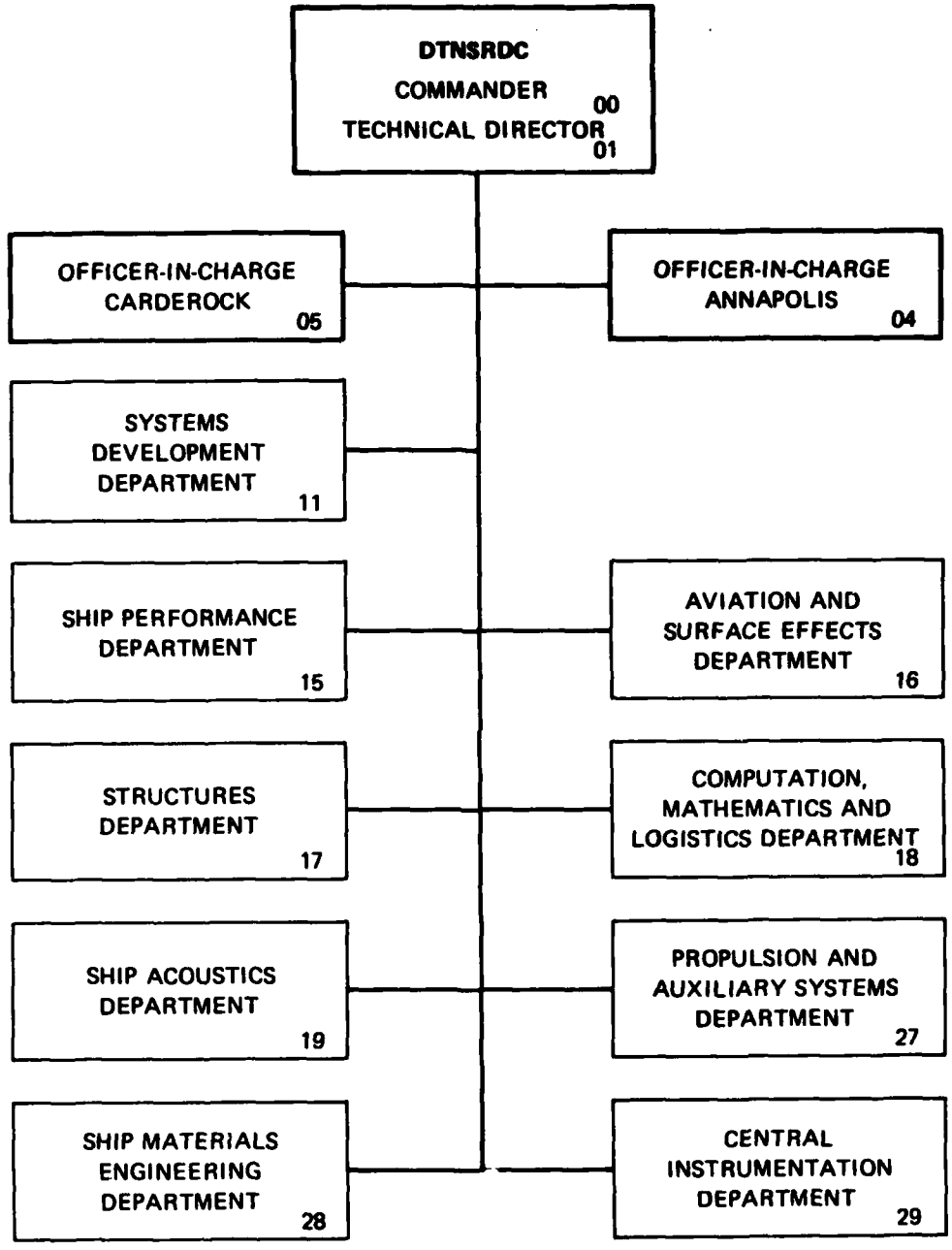

GPO 866 987

UNCLASSIFIED

SECURITY CLASSIFICATION OF THIS PAGE (When Data Entered)

REPORT DOCUMENTATION PAGE	READ INSTRUCTIONS BEFORE COMPLETING FORM
1. REPORT NUMBER: DTNSRDC/SPD-1018-01	2. GOVT ACCESSION NO.: AD-A126155
3. RECIPIENT'S CATALOG NUMBER	
4. TITLE (and Subtitle): THE DRAG OF A CIRCULAR CYLINDER ON OR NEAR A FLAT PLATE APPROPRIATE FOR SHIP-MODEL TURBULENCE STIMULATORS	5. TYPE OF REPORT & PERIOD COVERED
	6. PERFORMING ORG. REPORT NUMBER
7. AUTHOR(s): Chao-Ho Sung and Douglas S. Jenkins	8. CONTRACT OR GRANT NUMBER(s)
9. PERFORMING ORGANIZATION NAME AND ADDRESS: David W. Taylor Naval Ship Research and Development Center Bethesda, Md 20084	10. PROGRAM ELEMENT, PROJECT, TASK AREA & WORK UNIT NUMBERS: Program Element 62543N; Task Area 421-252; Work Unit 1507-201-33
11. CONTROLLING OFFICE NAME AND ADDRESS: Naval Sea Systems Command (05R) Washington, DC 20380	12. REPORT DATE: February 1983
	13. NUMBER OF PAGES: 56
14. MONITORING AGENCY NAME & ADDRESS(if different from Controlling Office)	15. SECURITY CLASS. (of this report): UNCLASSIFIED
	15a. DECLASSIFICATION/DOWNGRADING SCHEDULE

16. DISTRIBUTION STATEMENT (of this Report)

APPROVED FOR PUBLIC RELEASE: DISTRIBUTION UNLIMITED

17. DISTRIBUTION STATEMENT (of the abstract entered in Block 20, if different from Report)

18. SUPPLEMENTARY NOTES

19. KEY WORDS (Continue on reverse side if necessary and identify by block number)

Tripwire
Drag
Boundary Layer
Transition

20. ABSTRACT (Continue on reverse side if necessary and identify by block number)

Experiments were conducted to determine the drag coefficient C_D of the tripwire and the approximate location of boundary layer flow transition. The investigation was performed with a simplified model of a circular cylinder placed on or near a flat plate. The experimental conditions were those typical of ship-model appendage drag experiments. One of the purposes was to obtain a formula for C_D when there is a gap between the cylinder and the flat plate. An example of the drag prediction of an appendage, modeled as a flat plate, is

DD FORM 1 JAN 73 1473 EDITION OF 1 NOV 65 IS OBSOLETE
S/N 0102-LF-014-6601

UNCLASSIFIED

SECURITY CLASSIFICATION OF THIS PAGE (When Data Entered)

given based on the new C_D and the prediction method recommended here. A comparison with the result obtained using the prediction method currently in use at DTNSRDC is made. The results indicate that both the effect of a gap, if it exists, on the tripwire drag and the effect of the presence of the tripwire on the turbulent skin friction must be considered.

TABLE OF CONTENTS

LIST OF FIGURES

LIST OF TABLES

NOMENCLATURE

C_D	Pressure drag coefficient, defined in Equation [9]
C_D^*	Pressure drag coefficient normalized by that of an isolated cylinder at the same Reynolds number
C_L	Lift coefficient, defined in Equation [10]
$C_p(\theta)$	Local pressure coefficient at cylinder angle θ defined in Equation [8]
D	Sum of drags = $D_\ell + D_t + D_{T.W.}$
D_ℓ	Drag due to laminar skin friction
D_t	Drag due to turbulent skin friction
$D_{T.W.}$	Drag due to tripwire (T.W.)
k	Diameter of the circular cylinder (tripwire)
$P(\theta)$	Pressure at cylinder angle θ
P_s	Static pressure of the free stream
R_n	Cylinder Reynolds number, $R_n = Uk/\nu$
R_{n_k}	Roughness Reynolds number, $R_{n_k} = u_k k/\nu$; u_k is U at height k
U	Free stream flow velocity
u'	Velocity fluctuation
x	Distance in a direction parallel to the direction of flow
x_k	Distance from the leading edge to the location of the cylinder
x_o	Virtual origin of turbulence measured upstream of the location of the tripwire x_k
W	Width of the flat plate or length of the tripwire
δ	Thickness of the boundary layer
δ_k	Thickness of the boundary layer at the tripwire location x_k
δ_k^*	Displacement thickness of the boundary layer at the tripwire location x_k
$\theta(x)$	Momentum thickness of the boundary layer at the location x

ρ	Fluid density
ν	Kinematic viscosity of fluid

Subscripts

ℓ	Laminar boundary layer
t	Turbulent boundary layer

ABSTRACT

Experiments were conducted to determine the drag coefficient C_D of the tripwire and the approximate location of boundary layer flow transition. The investigation was performed with a simplified model of a circular cylinder placed on or near a flat plate. The experimental conditions were those typical of ship-model appendage drag experiments. One of the purposes was to obtain a formula for C_D when there is a gap between the cylinder and the flat plate. An example of the drag prediction of an appendage, modeled as a flat plate, is given based on the new C_D and the prediction method recommended here. A comparison with the result obtained using the prediction method currently in use at DTNSRDC is made. The results indicate that both the effect of a gap, if it exists, on the tripwire drag and the effect of the presence of the tripwire on the turbulent skin friction must be considered.

ADMINISTRATIVE INFORMATION

This work was authorized by the Office of Naval Technology, Ships, Subs and Boats Exploratory Development Program under the management of Naval Sea Systems Command (NAVSEA) (03R), and funded under Ship Performance Task Area 421-2652, administered by the Ship Performance Department of the David W. Taylor Naval Ship Research and Development Center (DTNSRDC), Work Unit Number 1507-201-33.

INTRODUCTION

The drag due to a tripwire used on a bare hull ship model constitutes only about 2 percent of the total drag. However, when a tripwire is used on a model appendage, its drag is in the order of 20 percent of the total drag of the appendage. Therefore, an accurate estimate of the drag caused by the presence of a tripwire is particularly important in model appendage drag experiments. The objectives of this investigation are to provide an accurate drag coefficient of the tripwire and to suggest an improved drag prediction method. The investigation

was conducted with a simplified model where a long circular cylinder was placed on or near a flat plate. The emphasis of the investigation is on determining the dependence of the drag coefficient of the tripwire on the Reynolds number, the location of the tripwire and, in particular, the gap between the tripwire and the flat plate.

A tripwire not only induces a drag, its presence also affects the structure of the boundary layer of the flat plate. Of special importance is its effect on the skin friction of the turbulent boundary layer downstream of the tripwire. The drag prediction method currently used at DTNSRDC ignores the latter effect. More specifically, this method makes the following assumptions: (1) the boundary layer transition occurs at the location of the tripwire, (2) the drag coefficient of the tripwire has a fixed value of 0.6, (3) the effect of the tripwire on the boundary layer is ignored and (4) the turbulent boundary layer is assumed to start at the location of the tripwire, i.e. the turbulent momentum thickness is assumed zero at that location.

The significance and the improvement of the four assumptions mentioned above are the main topics of discussion in this report. The discussion of the first two assumptions is based on the experimental results obtained here. The discussion of the last two assumptions is based on the drag prediction of a submarine sail which is modeled as a flat plate.

BACKGROUND

RANGES OF PARAMETERS

The pressure force on a tripwire can be decomposed into drag and lift. Drag is the component of the pressure force in the direction of the incoming free

stream and lift is the component perpendicular to it. The pressure force is a function of the free stream velocity, U, the kinematic viscosity ν, the diameter of the tripwire k, the distance of the location of the tripwire measured from the leading edge of the flat plate x_k and, finally, the gap between the tripwire and the flat plate g. Or,

$$\text{Drag (or Lift)} = f(g, k, x_k, U, \nu) \qquad [1]$$

Since length and time are the only fundamental units involved, three independent nondimensional parameters can be formulated from the five variables in Equation [1]. Although there are a number of ways to do this, the following parameters were selected,

$$\text{Drag (or Lift)} = f(g/k, x_k/k, Uk/\nu) \qquad [2]$$

Since the relative height of the tripwire and the boundary layer thickness at the location of the tripwire, δ_k, are also important parameters, an alternative form of Equation [2] is

$$\text{Drag (or Lift)} = f(g/k, k/\delta_k, Uk/\nu). \qquad [3]$$

The parameter $R_n = Uk/\nu$ will be called the cylinder Reynolds number hereafter.

The ranges of the three parameters in this investigation are chosen as

$$\begin{aligned} R_n &= 1{,}000, \quad 3{,}000, \quad 5{,}000, \quad 6{,}300 \\ x_k/k &= 24, 48, 124 \\ g/k &= 0.00, 0.5, 0.50, 1.00 \end{aligned} \qquad [4]$$

The ranges of R_n and x_k/k are those normally encountered in the model resistance experiments of bare hulls and appendages. In model resistance experiments, it may happen that the tripwire has a gap of one or more wire diameters. The upper limit of g/k for this investigation is chosen as unity, based on the results of previous investigations[1-3] at higher cylinder Reynolds numbers. It was found there that the drag on the cylinder ceases to increase with increasing gap when the gap is larger than one half of a diameter. A sketch of the geometry is shown in Figure 1.

TRANSITION

Predicted locations of natural flow transition on a flat plate relevant to this investiation are tabulated in Table 1. These calculations are based on the work of Wazzan[4,5]. The results indicate that although the onset of flow instability may occur within a distance of one hundred cylinder diameters downstream of the leading edge of the flat plate, natural transition occurs from several hundreds to several thousands of diameters downstream of the leading edge, depending on the intensity of free stream turbulence. Thus, natural transition does not occur on the plate within the experimental conditions listed in [4].

Several authors gave the criteria for the selection of a tripwire such that transition will occur at the location of the tripwire instantaneously. For example, Gibbings[6] gave a criterion as

$$R_n = Uk/\nu \gtrsim 826 \qquad [5]$$

and Preston[7] gave a criterion based on the roughness Reynolds number as

$$R_{n_k} = u_k k/\nu > 600, \qquad [6]$$

where u_k is the unperturbed velocity at the height of the tripwire when the tripwire is not there. On the other hand, Tani and Hama[8] concluded from their

investigation that transition can not take place instantly at the location of the tripwire; rather, it normally occurs at a certain distance downstream of the tripwire. A sketch of the transition due to a tripwire is shown in Figure 2. It is noted that in this example R_n = 644 and the ratio of the tripwire diameter to the displacement thickness k/δ_k^* is only 0.7. As a consequence, transition occurs 300 diameters downstream of the tripwire.

As it can be seen from Table 2, all the cases to be investigated have $k/\delta_k^* > 1$. Thus, not only criterion [5] is satisfied since the minimum R_n is 1000 but also criterion [6] is satisfied since, for $k/\delta_k^* > 1$, $u_k = U$. It is therefore to be expected that in all the cases to be investigated, transition should occur either instantaneously, or it should occur within a short distance downstream of the tripwire. The location of boundary layer transition will be investigated for the case where R_n=3,065, x_k/k=24 and g/k=0.

DRAG COEFFICIENT OF THE TRIPWIRE

For the case when there is no gap between the tripwire and the flat plate, several values for the drag coefficient of the tripwire, C_D, have been recommended in the past. Preston[7] suggested a value of 0.75 and Kozlov[9] gave a formula for C_D which depends on the roughness Reynolds number as

$$C_D = 2.6/(R_{n_k})^{1/2} + 0.6 \qquad [7]$$

The value of C_D currently used at DTNSRDC has a fixed value of 0.6.

When a model equipped with tripwire is towed in water, the interaction between the model surface and the tripwire generates a lift force which tends to push the tripwire away from the surface. If the tripwire is not securely attached

to the surface, this lift force can pull the wire away from the surface, leaving a gap between the tripwire and the model surface. The occurrence of such a gap has been observed after model resistance experiments. The effect of the gap on the value of C_D has not been investigated in the range of cylinder Reynolds numbers, R_n, for typical model tests, i.e. R_n = 1,000 - 6,000.

However, the effect of the gap on C_D has been investigated by several authors at higher cylinder Reynolds numbers. These Reynolds numbers vary from 2×10^4 to 2.5×10^5 which are from one to two orders of magnitude higher than those typical for ship model appendage tests. These authors include Bearman and Zdravkovich[1], Roshko et al.[2] and Goktun[3]. Their results vary slightly but have the same trend; that is, the value of C_D increases as the gap increases from zero until it reaches a critical gap of 0.3- 0.5 cylinder diameters. After this critical gap value, C_D remains constant as the gap increases further. The results of these investigations relevant to the present work are tabulated at the end of Table 3.

DESCRIPTION OF EXPERIMENTS

TEST FACILITY AND DATA ACQUISITION

The experiments were conducted in the Low Turbulence Wind Tunnel at DTNSRDC. A sketch of the experimental setup is shown in Figure 3.

Pressures were measured around the surface of the circular cylinder (i.e. tripwire) and were used to calculate the local pressure coefficient according to

$$C_p(\theta) = \frac{P(\theta) - P_S}{0.5\rho U^2}, \qquad [8]$$

where $P(\theta)$ is the pressure at cylinder angle θ, P_s is the static pressure of the free stream and ρ and U have the same meaning as before. The drag and the lift coefficient are then obtained as

$$C_D = 0.5 \int_0^{2\pi} C_p(\theta) \cos\theta \, d\theta \qquad [9]$$

and

$$C_L = 0.5 \int_0^{2\pi} C_p(\theta) \sin\theta \, d\theta \qquad [10]$$

respectively.

To determine the location of flow transition from laminar to turbulent flow, boundary layer velocity profiles were obtained with a one-component hot wire probe connected to a DISA Type 55M anemometer and a DISA Type M-10 linearizer.

DATA ACCURACY

To assure the accuracy of data, preliminary experiments were conducted to verify the following capabilities:

(1) the pressure around an isolated cylinder (i.e. without the interference from the flat plate) can be accurately measured,

(2) the flat plate is parallel to the direction of the free stream such that no leading edge separation nor pressure gradient is generated, and

(3) the wind tunnel blockage effect is less than 4 percent which implies less than 4 percent change in the measured value of C_D.

The largest deviation of the pressure gage output, when calibrated against a standard, was 0.5 percent of the maximum calibrated pressure of 690 Pa. In order

to check the repeatability of the pressure drag and lift coefficients, several experiments were repeated. The integrated pressure drag coefficients were repeatable within ± 6 percent except at the lowest speed where the drag coefficients were repeatable within ± 12 percent. At cylinder Reynolds numbers above 2,000, the lift coefficient repeated within ± 11 percent. At a Reynolds number less than 2,000, the lift coefficient varied by as much as a factor of two. However, in this case, the magnitude of the lift coefficient is on the order of 0.02 as compared to the maximum value of 0.5. The alignment of the cylinder angle with respect to the free stream direction was the most significant factor affecting the repeatability of the pressure drag and lift coefficients. The error in the alignment was less than ± 2.5 degrees. In comparison to the free stream velocity obtained by the pitot tube, the output from the hot wire probe when placed outside of the boundary layer agreed within ± 2 percent over a speed range of 1.0 to 8.0 m/s.

PRESENTATION AND DISCUSSION OF PRESSURE MEASUREMENTS

LOCAL PRESSURE COEFFICIENTS

Local pressure coefficients constitute the main body of the data base of this investigation. Since the main interest of this investigation is on drag coefficients, and to a lesser extent lift coefficients, the results of local pressure coefficients are presented in the Appendix.

DRAG COEFFICIENTS

As mentioned earlier, drag coefficient C_D depends on parameters R_n, x_k/k and g/k. The dependence of C_D on these parameters is the focus of the following discussions. The experimental results are tabulated in Table 3.

From Figures 4 to 6, it can be seen that the dependence of C_D on R_n is weak except at R_n = 1,000. This discrepancy is attributed to experimental difficulties at low Reynolds numbers.

The dependence of C_D on x_k/k at four gaps: g/k = 0., 0.25, 0.5 and 1. is illustrated in Figure 7. It is observed that the C_D-vs-x_k/k curve has approximately the same slope for all four gaps. The presently used C_D value at DINSRDC is also shown as a dotted line. The data were obtained under approximately the same experimental conditions but with no gap. The resulting C_D has a fixed value of 0.6 ± 0.1.

The reason for the dependency of C_D on x_k/k can be explained and will be given for the zero gap case at R_n = 3000. The fluid particles outside of the boundary layer carry larger kinetic energy than those inside the boundary layer. Therefore, if a larger portion of the tripwire extrudes outside the boundary layer, then a larger perturbation of the flow is expected and consequently, a larger drag of the tripwire is obtained. From Table 3, the ratios of the tripwire diameter to the boundary layer thickness at the location of the tripwire are k/δ_k = 2.3, 1.6 and 0.8 for x_k/k = 24, 48 and 124 respectively. Thus, at x_k/k = 24 two thirds of the tripwire is outside of the boundary layer while at x_k/k = 124, the tripwire is submerged completely inside the boundary layer. Thus, the C_D has a higher value of 0.6 at x_k/k = 24 but the value decreases to 0.41 at x_k/k = 124.

The dependence of C_D on g/k is presented in Figures 8 to 10. Allowing for different values of C_D at g/k = 0, all three C_D-vs-g/k curves at different tripwire locations have approximately the same shape as expected. To compare the results with those obtained at higher Reynolds numbers, the C_D-vs-g/k curve at

R_n=48,000 and x_k/k = 36 obtained by Bearman and Zdravkovich[1] is shown in Figure 11. The qualitative agreement is good.

An attempt was made to correlate the present results obtained here at R_n = 1000-6300 to those obtained at $R_n = 2x10^4 - 2.5 \times 10^5$ by Bearman and Zdravkovich[1], Roshko et al[2] and Goktun[3]. Since the value of C_D in the absence of the flat plate, i.e. the maximum C_D, is different depending on the value of R_n, drag coefficients C_D's are normalized by the maximum C_D at each R_n to facilitate the comparison at different R_n. The result is shown in Figure 12. As it can be seen, the correlation based on parameters k/δ_k and g/k is not quite satisfactory despite the fact that a systematic trend is there.

LIFT COEFFICIENTS

As can be expected, the variation of the lift coefficients is essentially the same as that of the drag coefficients and the discussion will not be repeated here. However, a discrepancy with the previous investigations obtained at higher Reynolds numbers should be pointed out.

Unlike previous investigations where all the lift coefficients are positive (cf. e.q. Figure 11), negative lift coefficients were obtained. Attempts to resolve the negative values have not been successful. However, since these negative values are rather small, their effects on the final result are probably not significant.

PRESENTATION AND DISCUSSION OF VELOCITY PROFILE MEASUREMENTS

The purpose of this portion of the investigation is to determine the actual location of flow transition when R_n = 3065, x_k/k = 24 and g/k = 0.

The mean velocity profiles are shown in Figure 13a while the fluctuations in the velocity profiles are shown in Figure 13b in terms of the turbulent intensity;

u'/U. At $x_k/k = 28$ and $x_k/k = 72$, in addition to the measured mean velocity profiles, the Blasius laminar profile and the turbulent velocity profile are included. The turbulent profile was determined from the 1/7-th power law relationship (cf. Schlichting[10]).

The fluctuations of the velocity immediately downstream of the cylinder follow a distinct pattern, as shown in Figure 13b. Four diameters downstream from the cylinder location, the turbulent intensity is approximately 0.1 percent in the absence of the cylinder. After the cylinder is placed on the flat plate, the turbulent intensity at $x_k/k = 28$ sharply increases to 8 percent near the surface of the plate. However, the fluctuations are mostly confined to a height less than three cylinder diameters. Eight diameters downstream of the cylinder ($x_k/k=32$), the peak of the intensity reaches 13 percent at approximately the height of the cylinder. As the fluctuations travel downstream, the peak intensity moves down toward the surface while fluctuations spread upward at the same time. At $x_k/k = 48$, the peak intensity near the plate surface is 8 percent, but the intensity at a height of three diameters is increased to approximately 2 percent. At $x_k/k = 72$, the intensity is uniformly distributed from the plate surface to a height of three diameters and it is on the order of 5 percent. The downward shift of the peak intensity of the fluctuations has also been observed by Tani and Sato.[11]

In summary, the separation region behind the cylinder extends beyond four cylinder diameters. The point of reattachment of the flow probably occurs between four and eight cylinder diameters downstream of the cylinder because the mean velocity near the plate surface goes from a negative value to a positive one at four and eight diameters downstream of the disturbance, respectively. Tani and Sato concluded that with k/δ_k^* greater than 0.64, transition occurs on top of the separated layer or soon after reattachment. Based on these results, transition

occurs at approximately eight diameters downstream of the cylinder. The flow may be considered to be completely turbulent 48 diameters downstream of the cylinder based on the velocity profile measurements. This conclusion is in agreement with Tani and Hama[8]; that is, transition cannot take place at the location of the cylinder despite the fact that the theoretical criterion for instantaneous transition as given in Equation [5] is satisfied.

However, since the velocity profile is quite different from that of the Blasius laminar flow, the assumption that the flow between the tripwire and the actual location of transition is turbulent appears to be adequate, at least as far as predicting skin friction is concerned.

A NEW DRAG COEFFICIENT OF THE TRIPWIRE

The derivation of the new drag coefficient of the tripwire is based on the pressure measurements discussed above. Three observations were made: (1) the dependence of C_D on R_n is weak, (2) the C_D-vs-x_k/k curves for different g/k have the same slope and (3) at a given x_k/k, C_D increases asymptotically as g/k increases until a critical value, somewhere between $g/k = 0.5$ and 1.0, is reached.

The first observation implies that $C_D = f(x_k/k, g/k)$ and the second observation provides the following empirical relationship from Figure 7.

$$\frac{C_{D_0} - C_D}{x_k/k - 24} = \frac{0.17}{124\text{-}24,} \qquad [11]$$

or

$$C_D = C_{D_0} - 0.0017\ (x_k/k - 24) \qquad [12]$$

where C_{D_0} is the drag coefficient at $x_k/k = 24$. The third observation implies that it is only necessary to consider $g/k \leq 1$ in order to determine C_{D_0} as a function of g/k.

From Table 3, the values of C_D at $x_k/k=24$, averaged over Reynolds numbers, are 0.62, 0.83, 0.96 and 1.1 for g/k = 0., 0.25, 0.5 and 1. respectively. Applying the third-degree Lagrange polynomial to make use of these four values, an equation for C_{D_0} as a function of g/k is obtained. This equation is substituted into [12] to give the new drag coefficient as

$$C_D = 0.62\ [1 + 1.7(g/k) - 1.4\ (g/k)^2 + 0.5\ (g/k)^3] \qquad [13]$$

$$- 0.0017\ (x_k/k - 24).$$

The ranges of parameters R_n, x_k/k and g/k for which the above formula is valid are those given in [4].

APPLICATION OF RESULTS: AN EXAMPLE

The two major results of the experimental investigation are: (a) a new tripwire drag coefficient is obtained and (b) although the flow transition occurs at a short distance downstream of the tripwire, the assumption that the flow between the tripwire and the transition point is turbulent appears to be a better approximation than assuming it is laminar. The following example illustrates the application of these results. A comparison of the predicted drag of a simplified appendage using the improved method and the method currently used at DTNSRDC is also made.

The current method used at DTNSRDC for the extrapolation of model drag data to full scale follows Froude's original method. The model residual drag is

obtained by subtracting from the measured total drag of the model the predicted drags due to laminar skin friction, turbulent skin friction and the tripwire. The residual drag coefficient thus obtained is then assumed to be the same for both the model and the full scale ship. In the case of submerged appended vehicles, the contribution of the wave resistance, which is Froude number dependent, to the residual drag is insignificant. Thus, the residual drag is mainly the contributions of form drags and the interference drags due to hull/ appendage junctions. Physical consideration indicates that both form drag and interference drag are Reynolds number dependent. Thus, the validity of the assumption that the residual drag coefficient is the same for both the model and the full scale ship depends on the validity of the assumption that both form drag and interference drag must be a weak function of the Reynolds number.

In the following example, an improved prediction method of the drag due to laminar skin friction, turbulent skin friction and the tripwire will be illustrated. A particular emphasis is to include the effect of a gap between the tripwire and the model surface on the drag of the tripwire and the effect of the presence of the tripwire on turbulent skin friction. To avoid unnecessary complications, the appendage will be simplified as a flat plate.

A typical sail modeled as a flat plate has a length of $L = 1.167$ ft and a width of $W = 0.695$ ft. A tripwire of diameter $k = 0.002$ ft is placed at 5 percent length downstream of the leading edge. The gap between the tripwire and the flat plate is assumed to have an average value of 0.5 diameter. The assumed value of 0.5 is for the purpose of illustrating the important effect of the gap; it may or may not actually occur in model tests. Then, at a towing speed of U

= 25.3 ft/sec, or 15 knots, the three parameters have the following values R_n = 4670, x_k/k = 29 and g/k = 0.5 which are within the conditions given in [4].

The total drag of the simplified model is the sum of the drags due to the tripwire $D_{T.W.}$, the laminar skin friction upstream of the tripwire D and the turbulent skin friction downstream of the tripwire D_t. The substitution of x_k/k = 29 and g/k = 0.5 into [13] gives C_D = 0.96. Assuming fresh water at 68°F, the drag due to the tripwire is

$$\begin{aligned} D_{T.W.} &= 1/2\,\rho U^2 \cdot kW \cdot C_D \\ &= 1/2\ (1.9364)\ (25.3)^2 (0.002)(\ 0.695)\ (0.96) \\ &= 0.83\ \text{lb} \end{aligned} \qquad [14]$$

The laminar boundary layer is assumed to have the Blasius solution, giving momentum thickness and skin friction as (cf. Schlichting[10], Chapter 7):

$$\theta_l(x) = 0.664\ (\nu x/U)^{1/2} = 0.664\ (\nu/U)^{1/2}\ x^{1/2} \qquad [15]$$

and

$$D_l(x) = \rho U^2 \cdot W \cdot \theta_l(x) \qquad [16]$$

respectively. Or,

$$\theta_l(x) = 4.3455 \cdot 10^{-4}\ x^{1/2}\ \text{ft} \qquad [15]'$$

$$D_\ell(x) = 0.3744 \cdot x^{1/2} \quad \text{lb} \qquad [16]'$$

Since $x = x_k = 5$ percent, $L = (0.05) \cdot (1.167) = 0.05835$ ft, [15]' and [16]' give $\theta_\ell(x_k) = 1.05 \cdot 10^{-4}$ ft and $D_\ell = D_\ell(x_k) = 0.09$ lb. The calculation of the turbulent boundary layer is somewhat more involved.

It will be assumed that the 1/7-th-power velocity distribution law holds for the turbulent boundary layer. Thus (cf. Schlichting[10], Chapter 21) for flat plate

$$\theta_t(x) = 0.036x \cdot (Ux/\nu)^{-1/5} = 0.036 \cdot (\nu/U)^{1/5} \cdot x^{4/5} \qquad [17]$$

and

$$D_t(x) = \rho U^2 W \theta_t(x) \; . \qquad [18]$$

Or,

$$\theta_t(x) = 19.17 \cdot 10^{-4} \cdot x^{4/5} \text{ ft}, \qquad [17]'$$

and

$$D_t(x) = 1.6416 \cdot x^{4/5} \text{ lb} \; . \qquad [18]'$$

It must be cautioned that x in [17] and [18] is the distance from the virtual origin of turbulence; not the distance from the location of the tripwire. The disturbances induced by the tripwire cause the momentum thickness to jump by a value proportional to the drag of the tripwire. The estimate of the jump will follow a suggestion by Preston[7] (see also a discussion by McCarthy et al.[12]).

Suppose the effect of the drag of the tripwire on momentum thickness is the same as that of the skin friction (i.e. Preston's assumption). Then according to [18], the jump of the momentum thickness at the location of the tripwire is related to the tripwire drag as

$$D_{T.W.} = \rho U^2 W \Delta\theta(x_k) \quad . \tag{19}$$

Thus, the momentum thickness of the turbulent boundary layer at x_k is

$$\theta_t(x_k) = \theta_\ell(x_k) + \Delta\theta(x_k) = \theta_\ell(x_k) + \frac{D_{T.W.}}{\rho U^2 W} \quad . \tag{20}$$

For the case considered here, $\theta_t(x_k) = (1.05 + 9.60)\times10^{-4}$ ft. The virtual origin is then given by [17]' as

$$x_0^{4/5} = \frac{10.65}{19.17\cdot10^{-4}} \quad , \text{ or } \quad x_0 = 0.48 \text{ ft} \quad . \tag{21}$$

It is cautioned that x_o is measured upstream starting from $x = x_k$. Finally, the drag due to the turbulent skin friction is the difference between the turbulent

skin friction from the virtual origin to the trailing edge of the plate and that from the virtual origin to the location of the tripwire:

$$D_t = 1.6516\ [(x_o + 95\%L)^{4/5} - x_o^{4/5}]$$

$$= 1.6516\ [(0.48+1.109)^{4/5} - (0.48)^{4/5}] = 1.47\ \text{lb} \quad [22]$$

The above results are summarized as Case A of Table 4.

The drag prediction method currently used at DTNSRDC has been described in the Introduction. The calculated results using this method are summarized as Case D of Table 4. A comparison with Case A indicates that the method used at DTNSRDC underestimates the drag due to the tripwire by 38 percent and overestimates the drag due to the turbulent skin friction by 22 percent. However, because of a fortuitous cancellation of errors, the sums of the drags in both cases are the same.

The above comparison is based on the assumption that there is a gap of g/k = 0.5 in Case A. The case where there is no gap so that $C_D = 0.6$ is used, but the effect of the tripwire drag on the turbulent skin friction drag is included is also considered here. These results are tabulated as Case B in Table 4. A comparison with Case D indicates that the current DTNSRDC method overestimates the turbulent skin friction by 15 percent, resulting in an overestimate of the sum of the drags by 11 percent.

There may be objections to the assumption that all the drag due to the tripwire has been converted to the jump in momentum thickness. Thus, [19] is modified as

$$\lambda D_{T.W.} = \rho U^2 W \cdot \Delta\theta(x_k), \quad 0<\lambda\leqslant 1 \quad [23]$$

To investigate the effect of the value of the factor λ on the predicted turbulent skin friction, the case $\lambda = 0.4$ will be considered. In this case, only 40 percent of the tripwire drag is converted to the jump in momentum thickness. The results are summarized as case C of Table 4. It is seen that the DTNSRDC method still overestimates the drag due to the turbulent skin friction by 11 pecent, assuming a gap $g/k = 0.5$.

If the assumption that $g/k = 0.5$ is reasonable, then the above comparisons indicate that the drag prediction method currently used at DTNSRDC is not adequate The degree of inadequacy will be less significant in ship model tests and more significant in small appendage model tests, such as sail planes. In all cases, the percentage errors will be less significant when other drag components, such as the form drag and the drag due to the hull/appendage junction, are included in the total drag.

SUMMARY AND RECOMMENDATIONS

The results of this investigation can be summarized by evaluating the assumptions made in the drag prediction method currently used at DTNSRDC. Descriptions of these assumptions are given in the Introduction. The evaluation is based on the drag prediction from the model test of a typical sail, simplified as a flat plate.

(a) The assumption that flow transition occurs at the location of the tripwire is adequate. Although this experimental investigation indicates that transition actually occurs at a short distance downstream of the tripwire, the flow between the tripwire and the actual transition point is quite different from that of the Blasius' laminar boundary layer. The assumption of a turbulent boundary layer is a better approximation.

(b) The assumption that $C_D = 0.6$ is not adequate when there is a gap between the tripwire and the model surface. For a gap of 0.5 tripwire diameter, the drag of the tripwire may be underestimated by 38 percent. Therefore, the use of a new drag coefficient of the tripwire, given in Equation [13], is recommended.

(c) The assumptions that the presence of the tripwire does not affect the boundary layer and that the virtual origin of turbulence occurs at the location of the tripwire are not adequate. 11 to 22 percent overestimate of the drag due to the turbulent skin friction can arise. Procedures of a more accurate drag prediction method are described in the previous section.

There are two uncertainties in the recommended drag prediction method: one is the value of the gap g/k and the other is the value of the factor λ in Equation [23]. Further investigations are needed to select values of g/k and λ appropriate for typical model test conditions.

Two improvements of the recommended method can also be made:

(i) A correction due to the curvature of the model surface should be made to modify the drag coefficient of the tripwire given by Equation [13].

(ii) Instead of the 1/7-th-power velocity distribution law, the log law of the wall should be used to improve the prediction of the turbulent skin friction.

ACKNOWLEDGEMENTS

The authors wish to acknowledge Messers. Robert Keller, Steve McGuigan and Dennis Mullinix for their assistance in setting up the experiment and the data acquisition system, and Mr. Victor Wu for this conscientious efforts in analyzing the pressure data and preparing many of the figures. Discussions with Dr. W.C. Lin, Mr. G. Dobay, and Mr. Bill Day are also acknowledged.

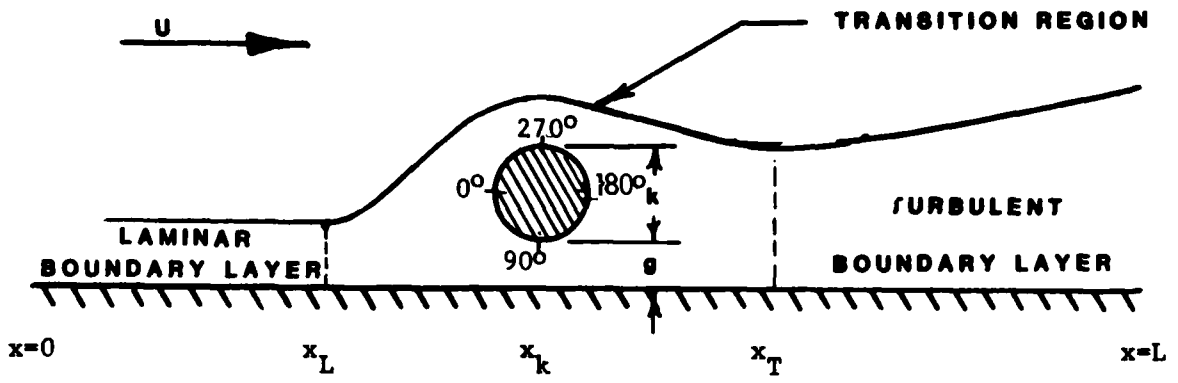

Figure 1 - Geometry of Cylinder Flat Plate System

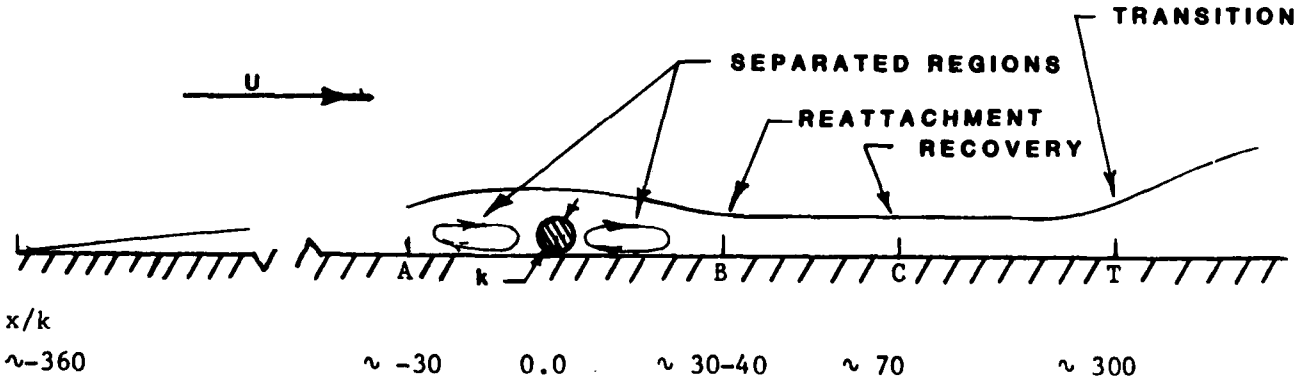

Figure 2 - Transition Due to a Tripwire
(R_n=644 and k/δ_k^*=0.7)

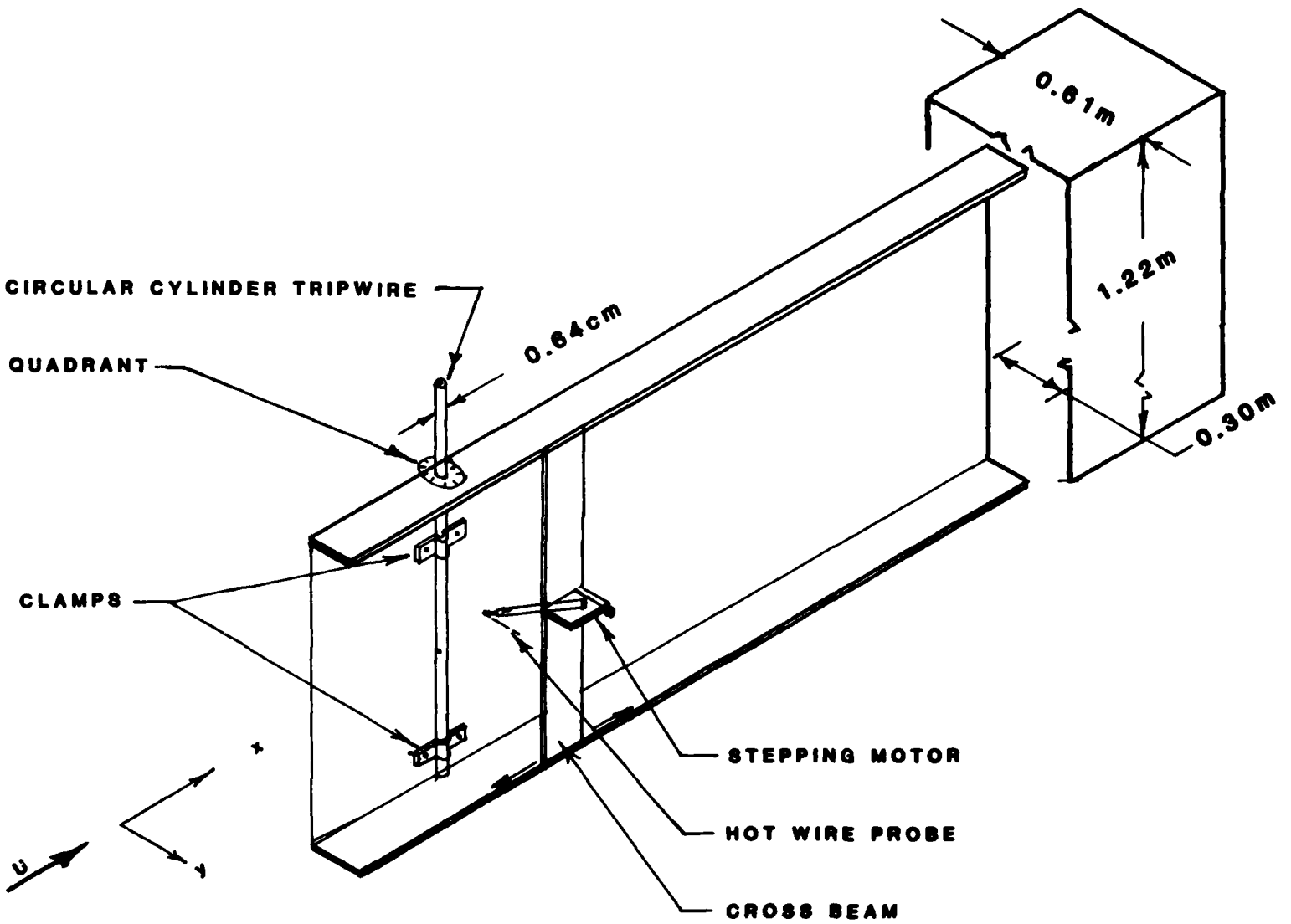

Figure 3 - Sketch of Experimental Setup

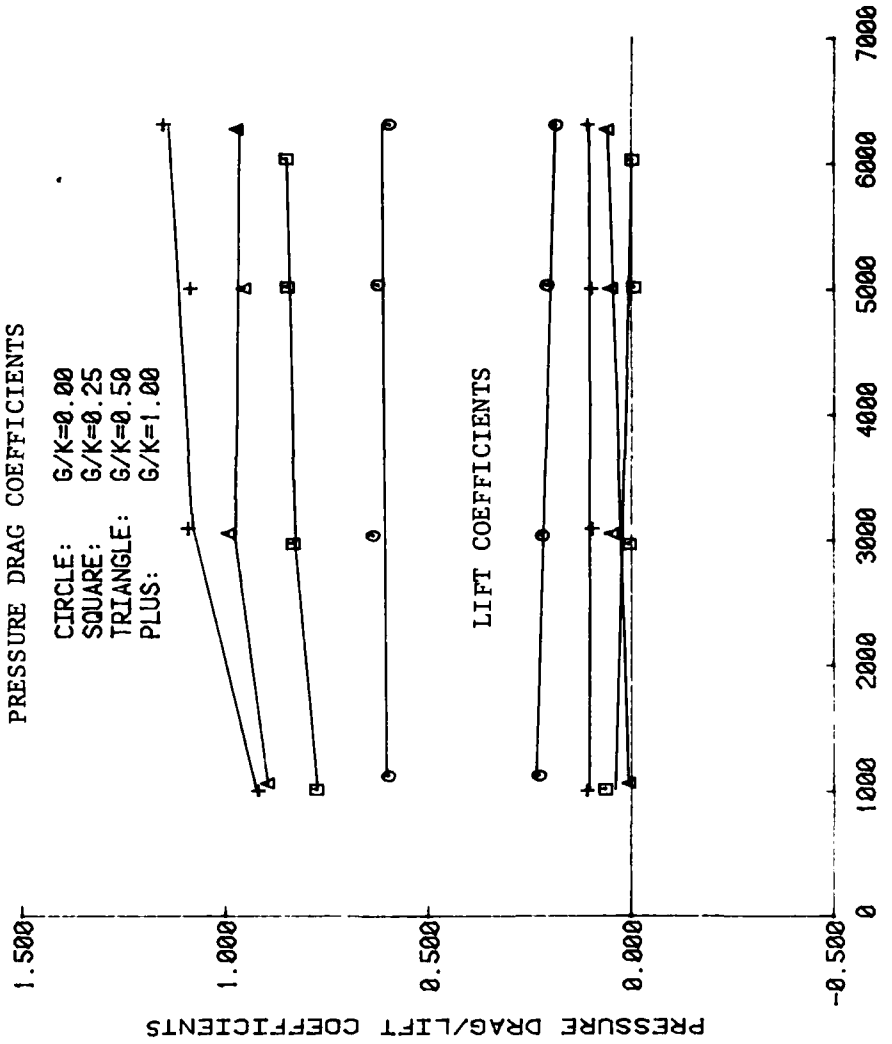

Figure 4 - Pressure Drag and Lift Coefficients versus Reynolds Number for Various Gaps at $x_k/k = 24$

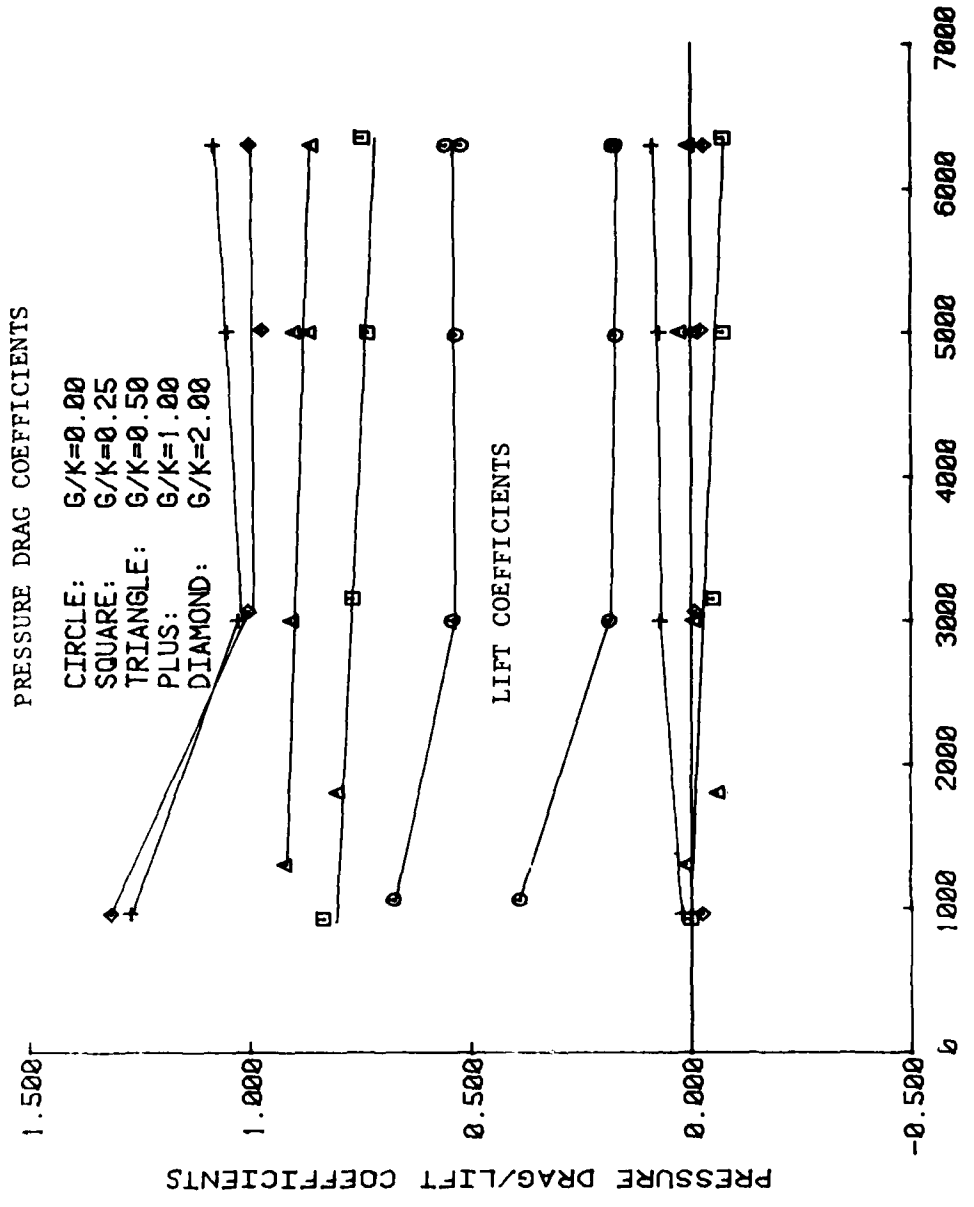

Figure 5 - Pressure Drag and Lift Coefficients versus Reynolds Number for Various Gaps at $x_k/k = 48$

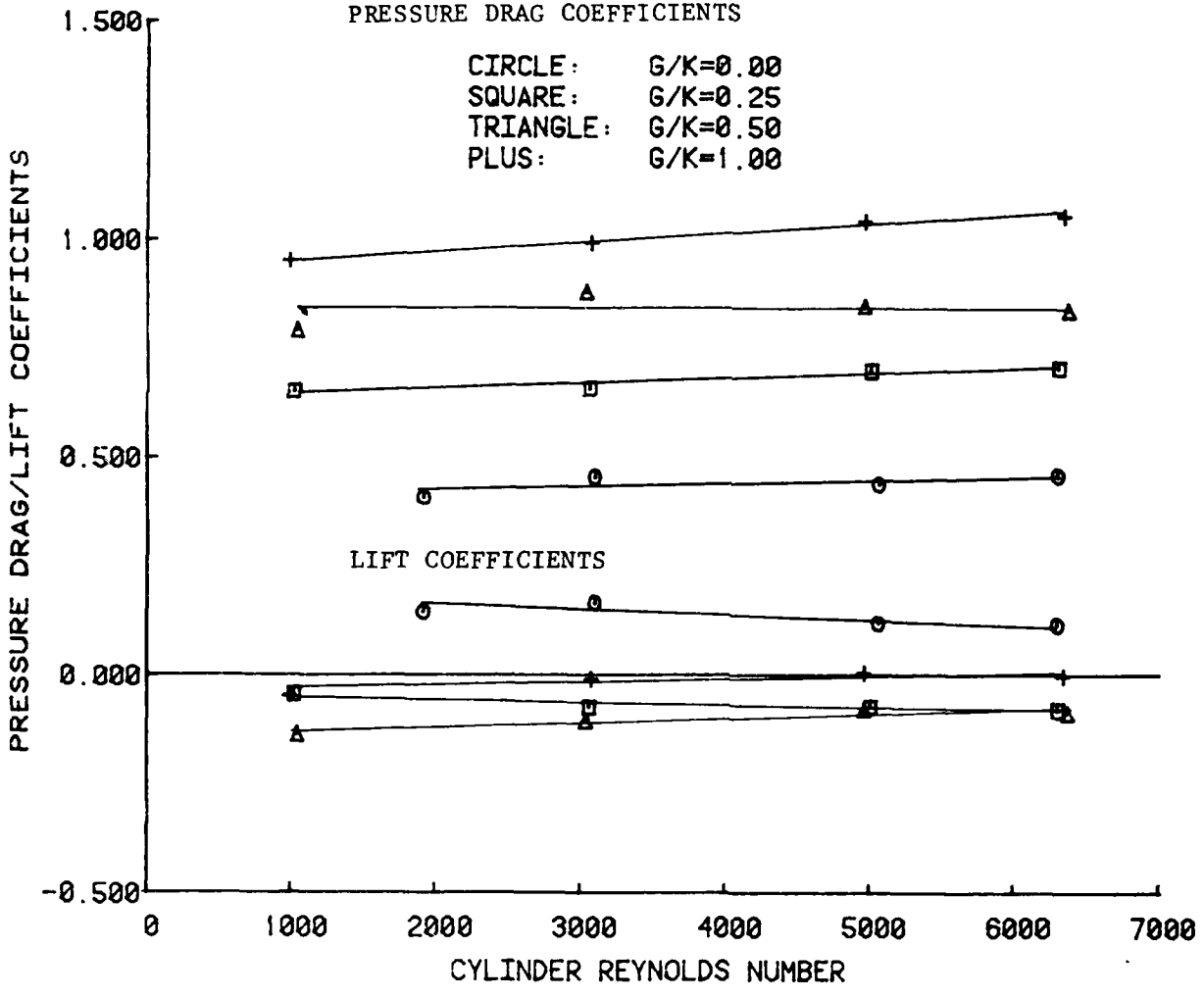

Figure 6 - Pressure Drag and Lift Coefficients versus Reynolds Number for Various Gaps at $x_k/k = 124$

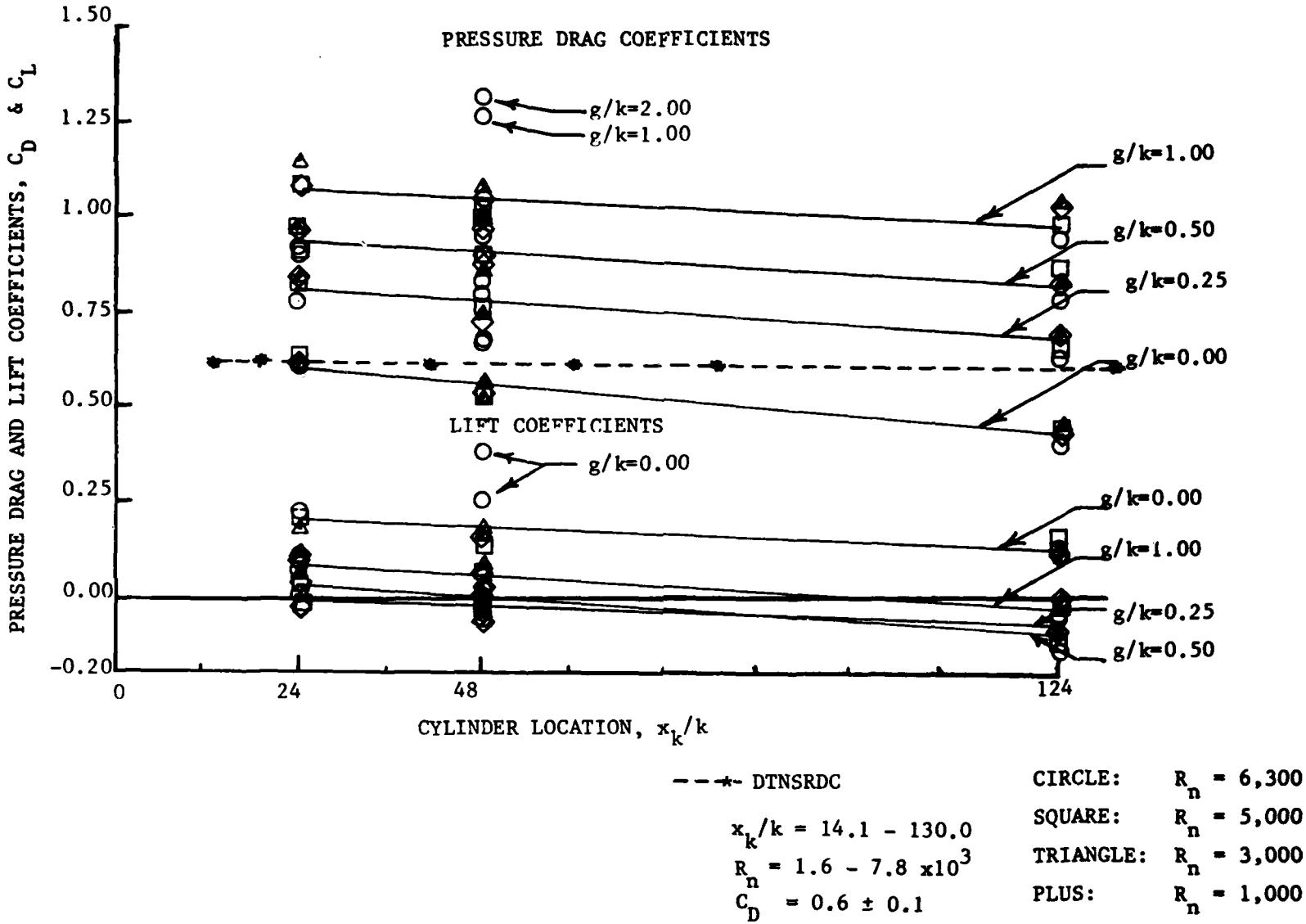

---*--- DTNSRDC

x_k/k = 14.1 - 130.0

R_n = 1.6 - 7.8 x10^3

C_D = 0.6 ± 0.1

CIRCLE: R_n = 6,300

SQUARE: R_n = 5,000

TRIANGLE: R_n = 3,000

PLUS: R_n = 1,000

Figure 7 - Pressure Drag and Lift Coefficients versus Cylinder Location for Various Reynolds Numbers and Gaps

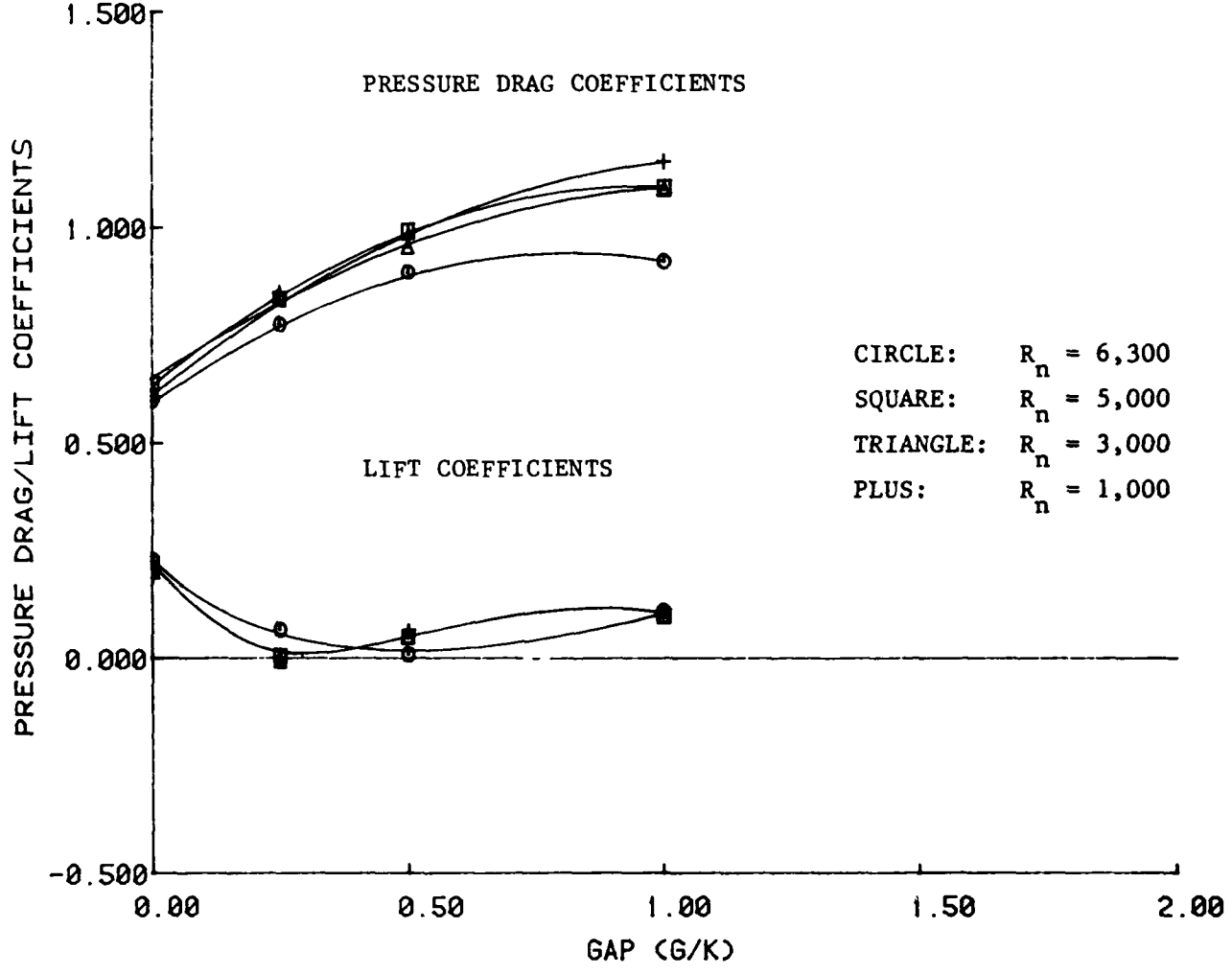

Figure 8 - Pressure Drag and Lift Coefficients versus Gap for Various Reynolds Numbers at $x_k/k = 24$

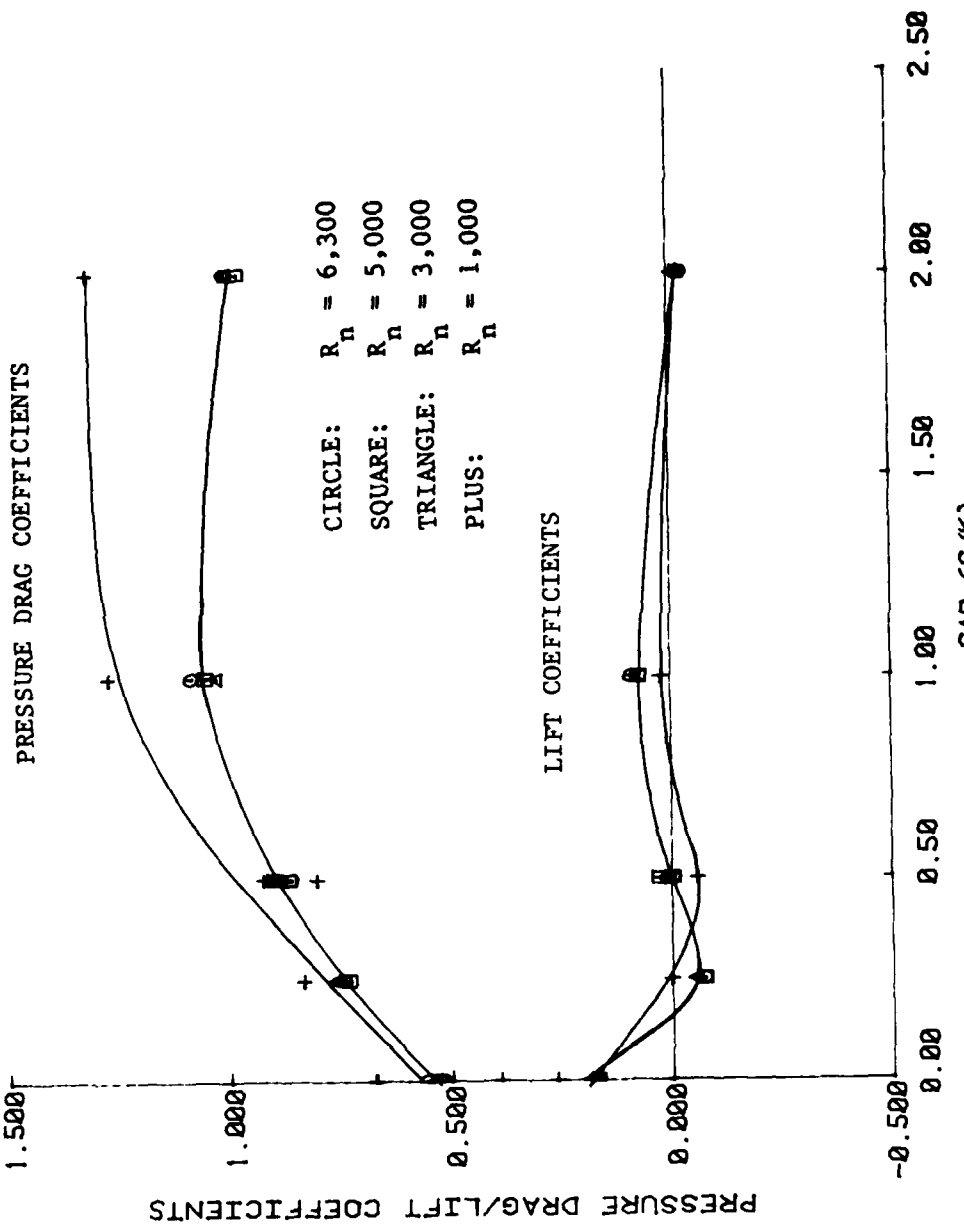

Figure 9 - Pressure Drag and Lift Coefficients versus Gap for Various Reynolds Numbers at x_k/k = 48

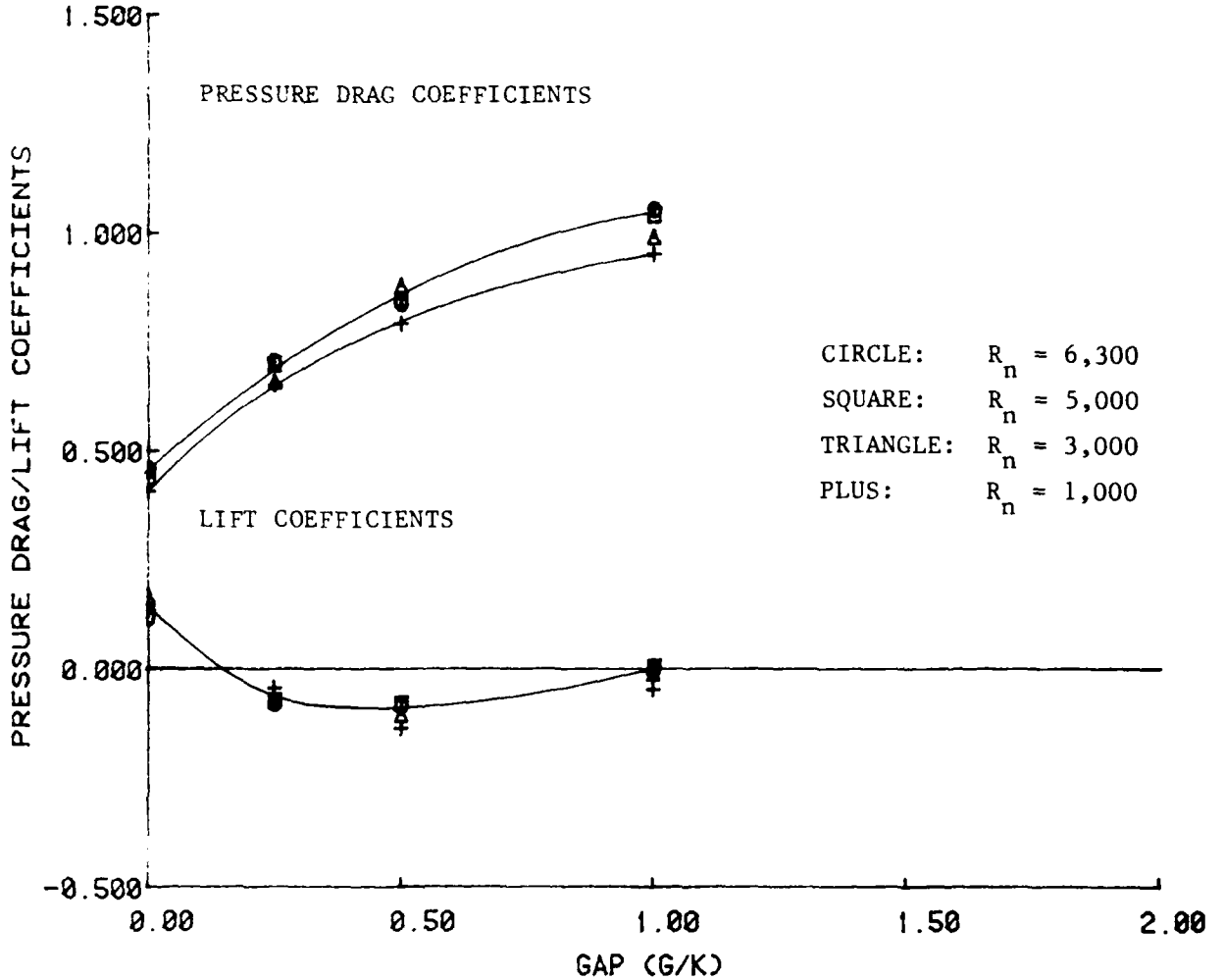

Figure 10 - Pressure Drag and Lift Coefficients versus Gap for Various Reynolds Numbers at $x_k/k = 124$

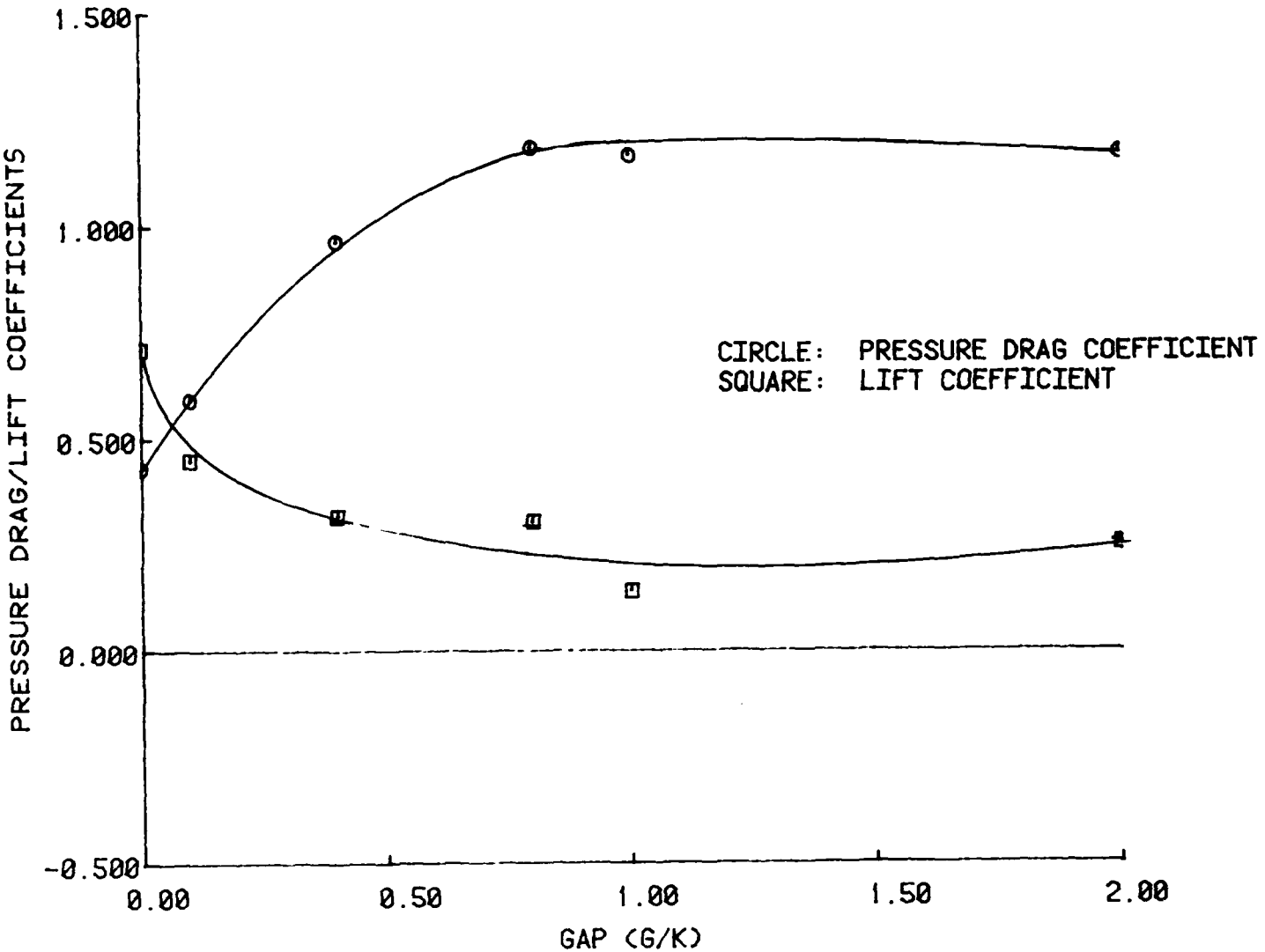

Figure 11 - Pressure Drag and Lift Coefficients versus Gap at $x_k/k = 36$ and $R_n = 48,000$ by Bearman and Zdravkovich[1]

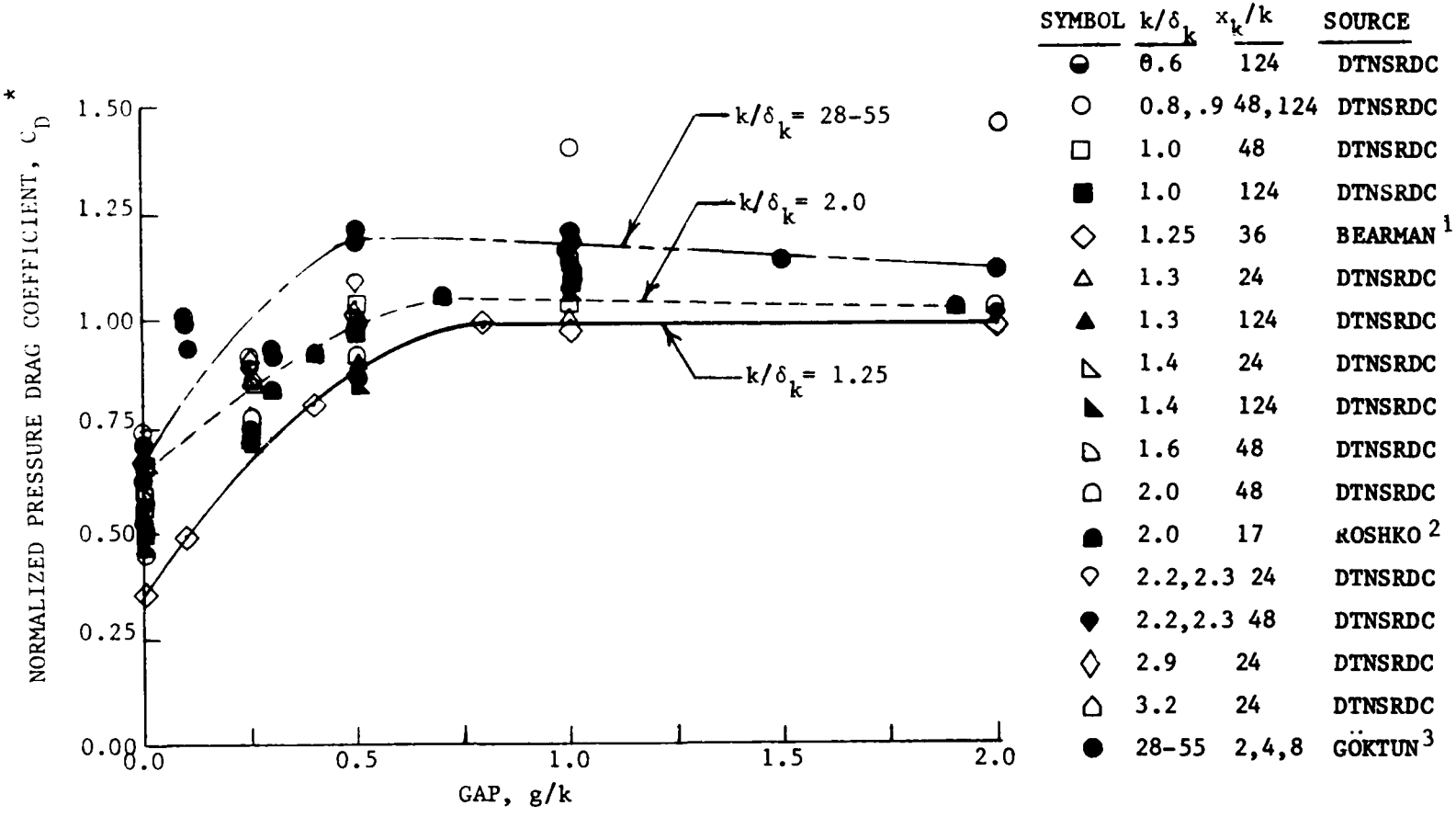

SYMBOL	k/δ_k	x_k/k	SOURCE
◒	0.6	124	DTNSRDC
○	0.8, .9	48, 124	DTNSRDC
□	1.0	48	DTNSRDC
■	1.0	124	DTNSRDC
◇	1.25	36	BEARMAN [1]
△	1.3	24	DTNSRDC
▲	1.3	124	DTNSRDC
◺	1.4	24	DTNSRDC
◣	1.4	124	DTNSRDC
⬠	1.6	48	DTNSRDC
⬡	2.0	48	DTNSRDC
⬢	2.0	17	KOSHKO [2]
◇	2.2, 2.3	24	DTNSRDC
◆	2.2, 2.3	48	DTNSRDC
◇	2.9	24	DTNSRDC
⬠	3.2	24	DTNSRDC
●	28-55	2, 4, 8	GÖKTUN [3]

Figure 12 - Normalized Pressure Drag Coefficient versus Gap for Various k/δ_k

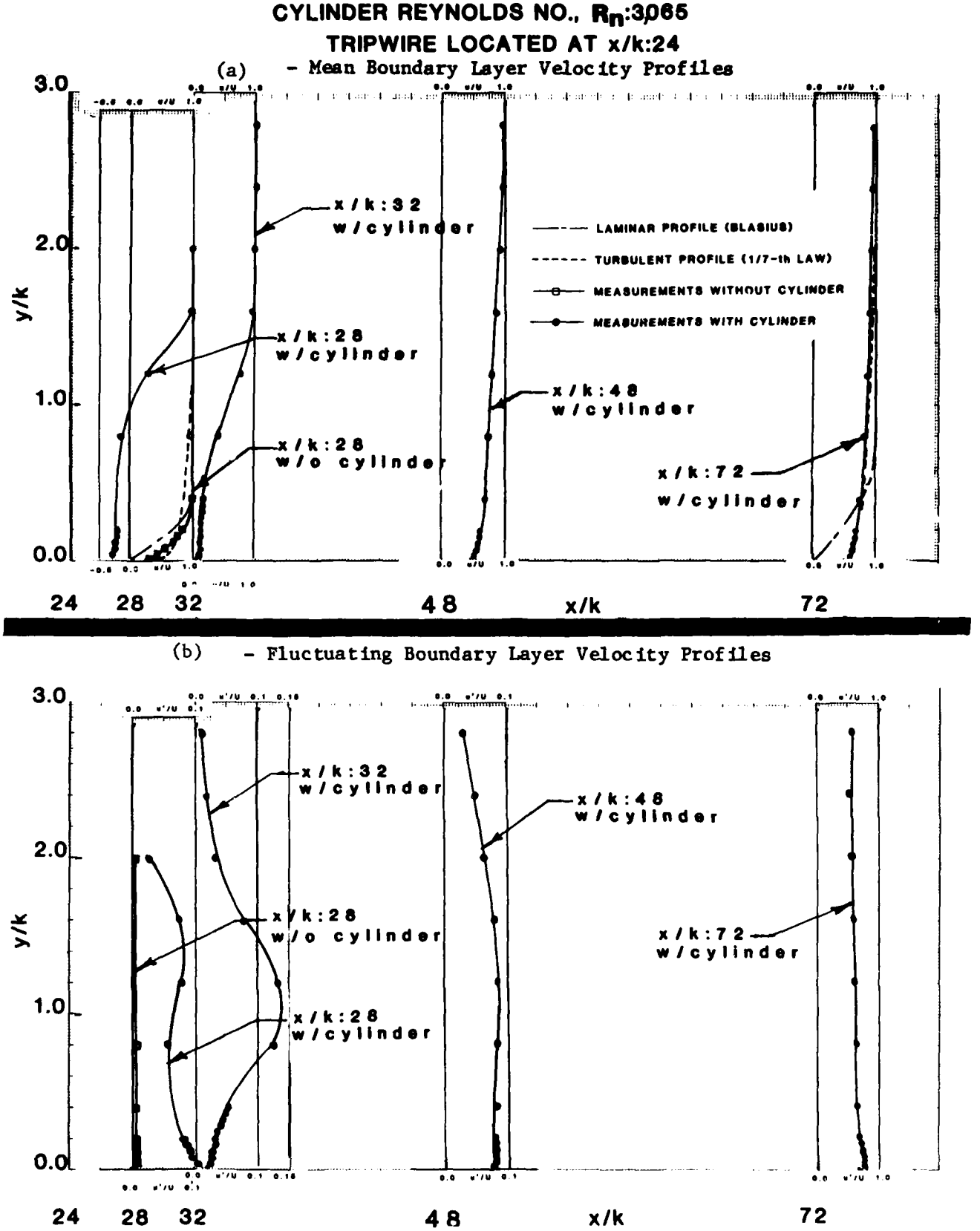

Figure 13 - Variations of (a) Mean Boundary Layer and (b) Fluctuating Boundary Layer Velocity Profiles

TABLE 1 - PREDICTED LOCATION OF THE ONSET OF INSTABILITY (CRITICAL) AND TRANSITION IN CYLINDER DIAMETERS DOWNSTREAM FROM THE LEADING EDGE OF A FLAT PLATE

(Calculations based on the work of Wazzan[11,12])

Flow Speed (m/s)	R_n	R_{n_L} =10^5 critical	R_{n_L} =5×10^6* transition	R_{n_L} =10^6** transition
2.4	1,000	97	4,856	931
7.0	3,000	33	1,665	333
11.6	5,000	20	1,005	201
14.7	6,300	16	783	156

*Intensity of free stream turbulence is 0.02 percent

**Intensity of free stream turbulence is 0.8 percent

TABLE 2 - RATIO OF CYLINDER HEIGHT TO DISPLACEMENT THICKNESS OF BLASIUS LAMINAR BOUNDARY LAYER (k/δ_k^*)

R_n \ x_k/k	24	48	124
1000	3.8	2.7	1.7
3000	6.5	4.6	2.9
5000	8.4	5.9	3.7
6300	9.4	6.7	4.1

where,

$$k/\delta_k^* = 0.5811\sqrt{R_n(x_k/k)}$$

TABLE 3 - SUMMARY OF EXPERIMENTAL RESULTS FOR PRESSURE MEASUREMENTS

Experiment No.	x_k/k	$R_n \times 10^3$	k/δ_k	g/k	C_D	C_L	C_D *
83	24	1.1	1.4	0.00	0.60	0.23	0.66
87	24	1.0	1.3	0.25	0.78	0.07	0.86
91	24	1.1	1.3	0.50	0.90	0.01	0.99
95	24	1.0	1.3	1.00	0.92	0.11	1.00
82	24	3.0	2.3	0.00	0.64	0.22	0.70
86	24	3.0	2.2	0.25	0.83	0.00	0.91
90	24	3.1	2.3	0.50	0.99	0.05	1.09
94	24	3.1	2.3	1.00	1.09	0.10	1.20
81	24	5.0	2.9	0.00	0.62	0.21	0.65
85	24	5.0	2.9	0.25	0.85	-0.01	0.90
89	24	5.0	2.9	0.50	0.96	0.05	1.01
93	24	5.0	2.9	1.00	1.09	0.10	1.15
80	24	6.3	3.2	0.00	0.60	0.18	0.60
84	24	6.3	3.2	0.25	0.85	0.00	0.85
88	24	6.3	3.2	0.50	0.97	0.06	0.97
92	24	6.3	3.2	1.00	1.15	0.11	1.15
30	48	1.1	0.9	0.00	0.67	0.39	0.74
29	48	1.3	1.0	0.00	0.68	0.26	0.75
49	48	1.0	0.9	0.25	0.84	0.00	0.92
45	48	1.3	1.0	0.50	0.95	0.02	1.04
43	48	1.8	1.2	0.50	0.80	-0.06	0.88
54	48	1.0	0.9	1.00	1.27	0.02	1.40
59	48	1.0	0.9	2.00	1.32	-0.02	1.45
27	48	3.0	1.6	0.00	0.54	0.14	0.59
33	48	3.2	1.6	0.25	0.77	-0.05	0.85
41	48	3.0	1.6	0.50	0.91	0.00	1.00
51	48	3.0	1.6	1.00	1.03	0.07	1.13
58	48	3.1	1.6	2.00	1.00	-0.01	1.10
28	48	5.0	2.0	0.00	0.53	0.17	0.56
32	48	5.0	2.0	0.25	0.73	-0.07	0.77
40	48	5.0	2.0	0.50	0.90	0.03	0.95

TABLE 3 -(CONTINUED)

Experiment No.	x_k/k	$R_n \times 10^3$	k/δ_k	g/k	C_D	C_L	C_D *
44	48	5.0	2.0	0.50	0.87	0.00	0.92
52	48	5.0	2.0	1.00	1.05	0.07	1.11
57	48	5.0	2.0	2.00	0.97	-0.02	1.02
25	48	6.3	2.3	0.00	0.56	0.17	0.56
26	48	6.3	2.3	0.00	0.52	0.18	0.52
31	48	6.4	2.3	0.25	0.75	-0.07	0.75
39	48	6.3	2.3	0.50	0.86	0.01	0.86
53	48	6.3	2.3	1.00	1.08	0.09	1.08
56	48	6.3	2.3	2.00	1.00	-0.03	1.00
65	124	1.9	0.8	0.00	0.41	0.14	0.45
70	124	1.0	0.6	0.25	0.65	-0.04	0.71
79	124	1.1	0.6	0.50	0.79	-0.14	0.87
74	124	1.0	0.6	1.00	0.95	-0.05	1.10
63	124	3.1	1.0	0.00	0.45	0.17	0.50
69	124	3.1	1.0	0.25	0.66	-0.07	0.73
77	124	3.0	1.0	0.50	0.88	-0.11	0.97
73	124	3.1	1.0	1.00	0.99	-0.01	1.09
62	124	5.1	1.3	0.00	0.44	0.12	0.46
68	124	5.0	1.3	0.25	0.70	-0.07	0.74
75	124	5.0	1.3	0.50	0.85	-0.08	0.90
72	124	5.0	1.3	1.00	1.04	0.00	1.10
60	124	6.3	1.4	0.00	0.46	0.12	0.46
67	124	6.3	1.4	0.25	0.70	-0.08	0.70
76	124	6.4	1.4	0.50	0.84	-0.09	0.84
71	124	6.3	1.4	1.00	1.05	0.00	1.05

TABLE 3 - (CONTINUED)

Experiment No.	x_k/k	$R_n \times 10^3$	k/δ_k	g/k	C_D	C_L	C_D^*
Bearman et. al.	36	48.0	1.25	0.0	0.43	0.71	0.36
	36	48.0	1.25	0.1	0.59	0.45	0.49
	36	48.0	1.25	0.4	0.96	0.32	0.80
	36	48.0	1.25	0.8	1.18	0.30	0.98
	36	48.0	1.25	1.0	1.16	0.14	0.97
	36	48.0	1.25	2.0	1.17	0.25	0.98
Roshko et. al.	17	20.0	2.0	0.0	0.79	0.60	0.66
	17	20.0	2.0	0.3	1.00	0.16	0.83
	17	20.0	2.0	0.4	1.10	0.12	0.92
	17	20.0	2.0	0.7	1.26	0.08	1.05
	17	20.0	2.0	1.0	1.24	0.03	1.03
	17	20.0	2.0	1.9	1.22	0.01	1.02
Göktun	4	90.0	30	0.0	0.85	1.30	0.71
	4	90.0	30	0.1	1.16	0.40	0.97
	4	90.0	30	0.3	1.12	0.25	0.93
	4	90.0	30	0.5	1.41	0.12	1.18
	4	90.0	30	1.0	1.39	0.06	1.16
	4	90.0	30	1.5	1.35	0.02	1.13
	4	90.0	30	2.0	1.32	0.01	1.10
	8	153.0	28	0.0	0.63	1.20	0.53
	8	153.0	28	0.1	1.12	0.30	0.93
	8	153.0	28	0.3	1.09	0.22	0.91
	8	153.0	28	0.5	1.45	0.10	1.21
	8	153.0	28	1.0	1.41	0.06	1.18
	8	153.0	28	1.5	1.36	0.04	1.13
	8	153.0	28	2.0	1.33	0.03	1.11
	4	153.0	39	0.0	0.64	1.44	0.53
	4	153.0	39	0.1	1.16	0.41	0.97
	4	153.0	39	0.3	1.09	0.28	0.91
	4	153.0	39	0.5	1.46	0.10	1.22
	4	153.0	39	1.0	1.44	0.06	1.20
	4	153.0	39	1.5	1.35	0.04	1.13
	4	153.0	39	2.0	1.33	0.03	1.11
	2	153.0	55	0.0	0.75	1.58	0.63
	2	153.0	55	0.1	1.21	0.42	1.01
	2	153.0	55	0.3	1.11	0.29	0.93
	2	153.0	55	0.5	1.46	0.10	1.22
	2	153.0	55	1.0	1.44	0.06	1.20
	2	153.0	55	1.5	1.35	0.04	1.13
	2	153.0	55	2.0	1.33	0.03	1.11

TABLE 4 - COMPARISON OF DRAG PREDICTION METHODS*

Case	Drag Coeff. C_D	Momentum Thickness at x_k ($\times 10^4$ ft)			Virtual Origin*** x_o(ft)	Drag (lb)			
		Laminar	T.W.** Induced	Turbulent		Laminar D	Turbulent D_t	T.W. $D_{T.W.}$	Sum D
A	0.96	1.05	9.60	10.65	0.48	0.09 (4%)	1.47 (61%)	0.83 (39%)	2.39
B	0.60	1.05	6.04	7.09	0.29	0.09 (4%)	1.55 (72%)	0.52 (24%)	2.16
C	0.96	1.05	3.80	4.85	0.18	0.09 (3%)	1.61 (64%)	0.83 (33%)	2.52
D	0.60	1.05	0	0	0	0.09 (4%)	1.79 (75%)	0.52 (21%)	2.40

* Predictions are based on a flat plate of length 1.167 ft and width 0.695 ft with a tripwire of diameter k = 0.002 ft placed at 5% plate length downstream of the plate leading edge and the gap between the plate and the tripwire is 0.5k. Thus, R_n = 4670, x_k/k = 29 and g/k=0.5 The skin friction drags of the laminar and the turbulent flow are based on the Blasius solution and the 1/7-th-power velocity distribution law respectively.

** T.W. = Tripwire

*** The virtual origin of the turbulent boundary layer is measured upstream from $x=x_k$.

Case A: C_D obtained from Equation (13) and the effect of $D_{T.W.}$ on the boundary layer is included (λ=1).

Case B: C_D = 0.60 (no gap) and the effect of $D_{T.W.}$ on the boundary layer is included (λ=1).

Case C: C_D obtained from Equation (13), but only the effect of 40% $D_{T.W.}$ on the boundary layer is included.

Case D: This is the prediction method currently used at DTNSRDC. Here, C_D has a fixed value of 0.60, the effect of $D_{T.W.}$ on the boundary layer is not included and the origin of turbulence is assumed to be at x_k, i.e. $\theta(x_k) = 0$.

APPENDIX A

FIGURES OF LOCAL PRESSURE COEFFICIENTS

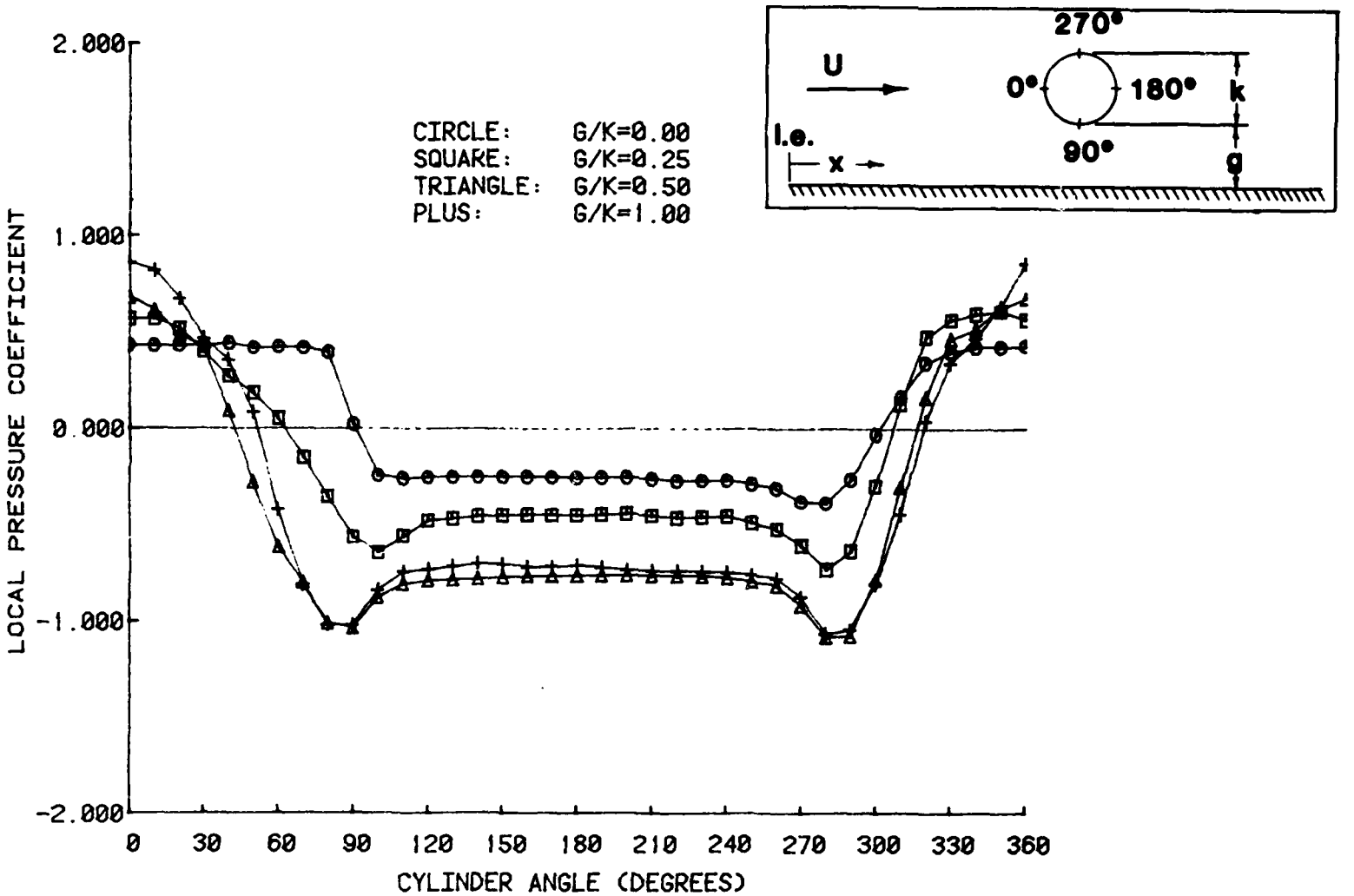

Figure A-1. Local Pressure Coefficient versus Cylinder Angle for Various Gaps ($x_k/k=24$, $R_n=1,000$)

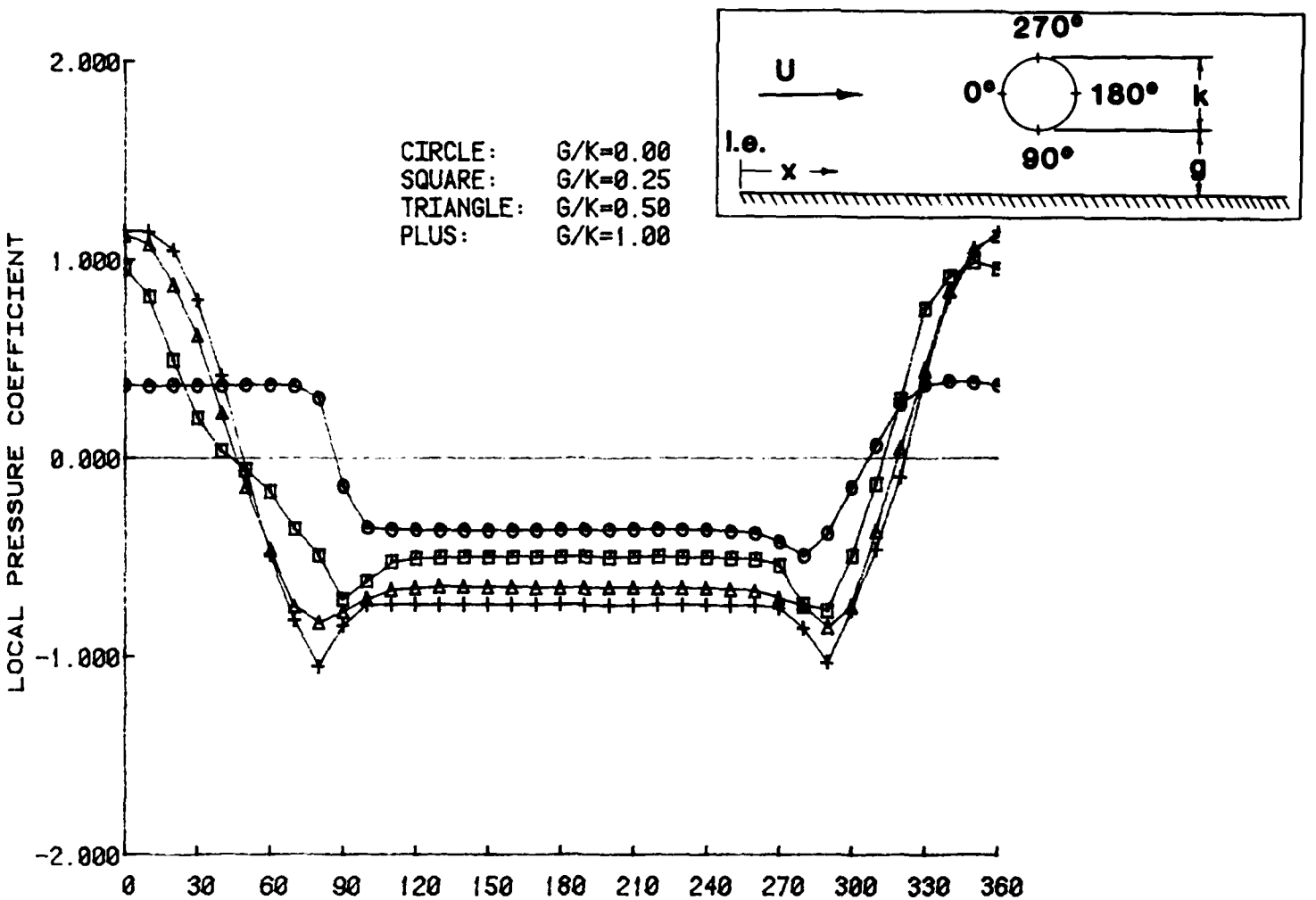

Figure A-2- Local Pressure Coefficient versus Cylinder Angle for Various Gaps ($x_c/k=24$, $R_D=3,000$)

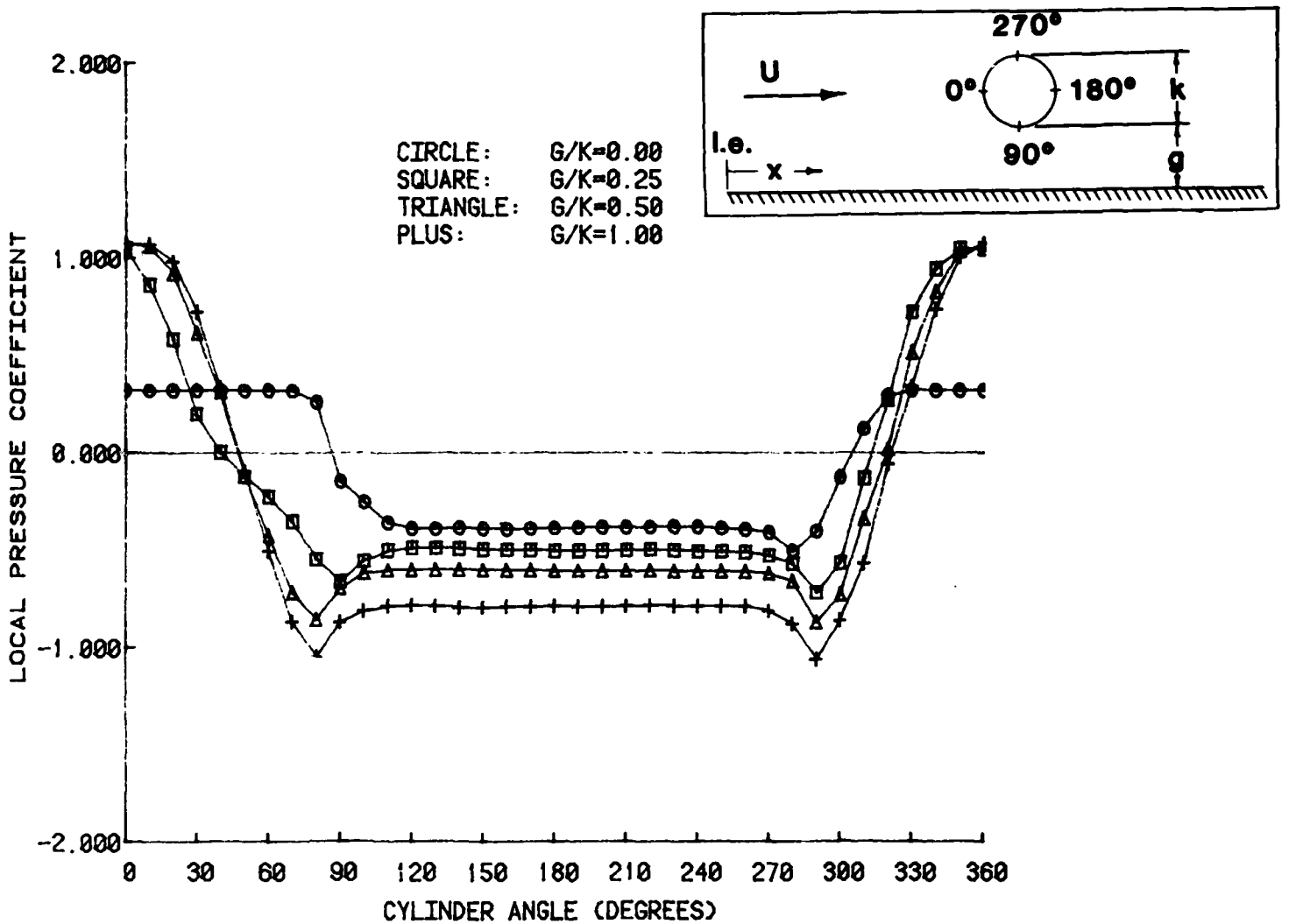

Figure A-3- Local Pressure Coefficient versus Cylinder Angle for Various Gaps ($x_k/k=24$, $R_n=5,000$)

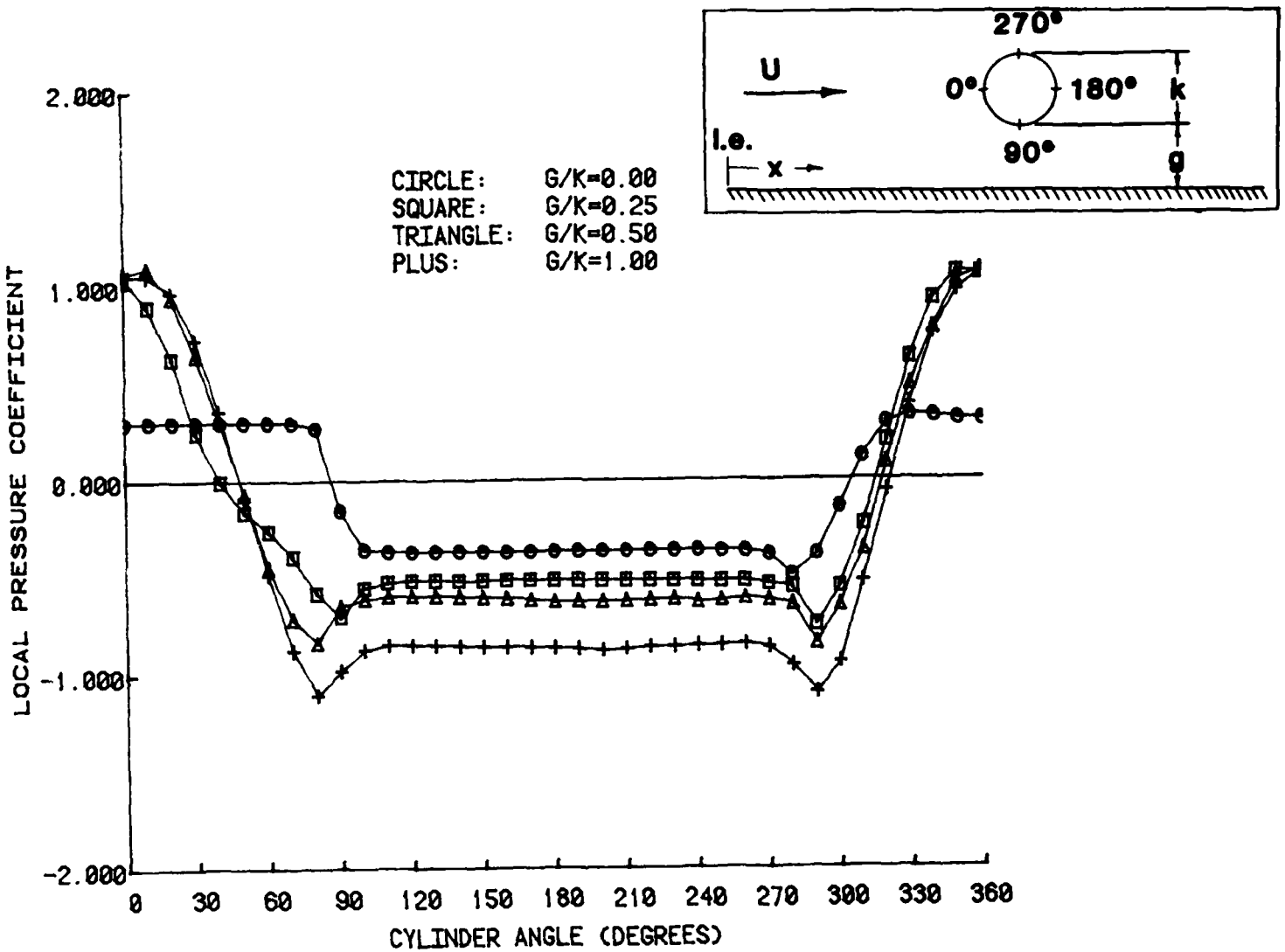

Figure A-4- Local Pressure Coefficient versus Cylinder Angle for Various Gaps ($x_k/k=24$, $R_n=6,300$)

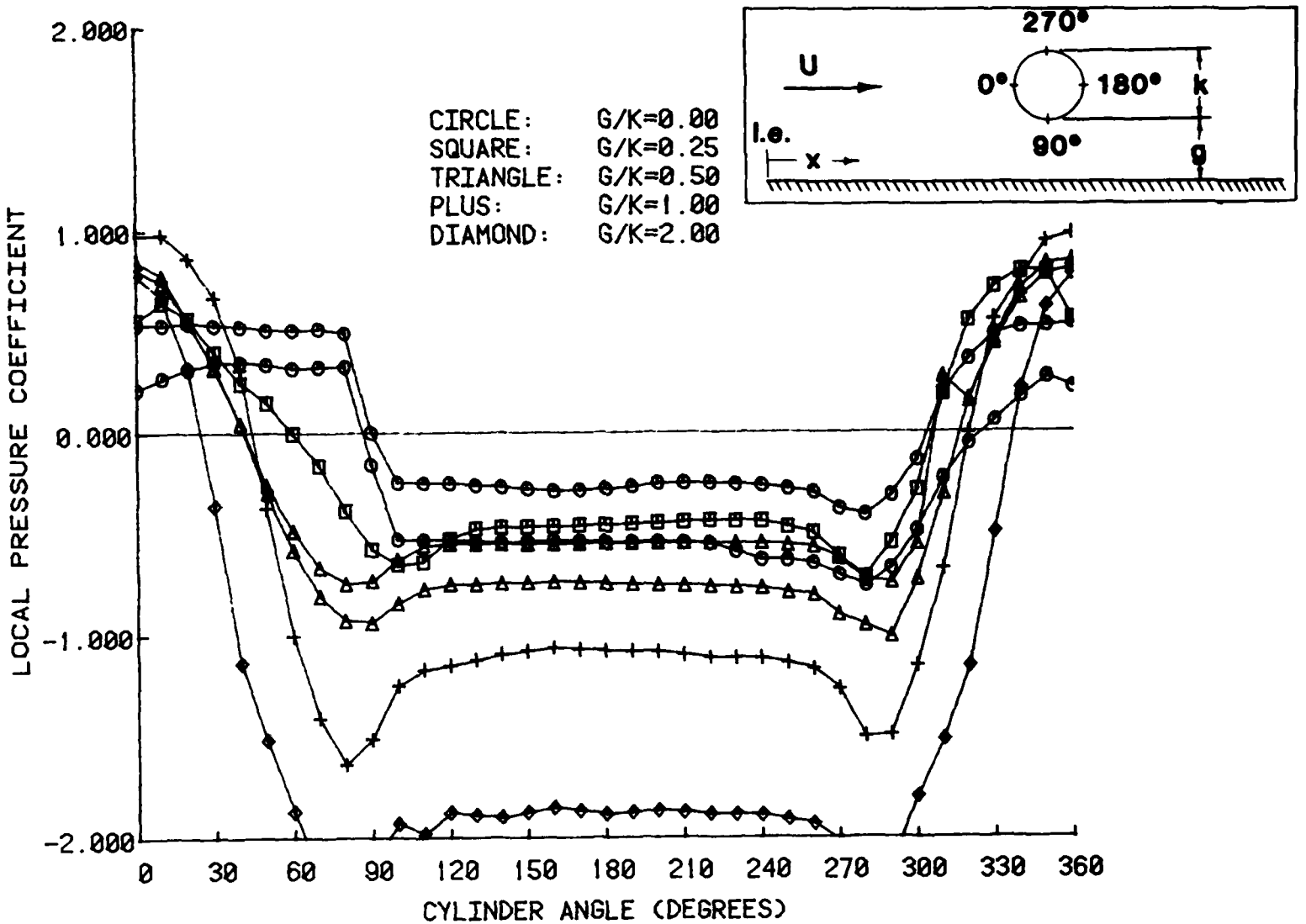

Figure A-5- Local Pressure Coefficient versus Cylinder Angle for Various Gaps ($x_k/k=48$, $R_n=1,000$)

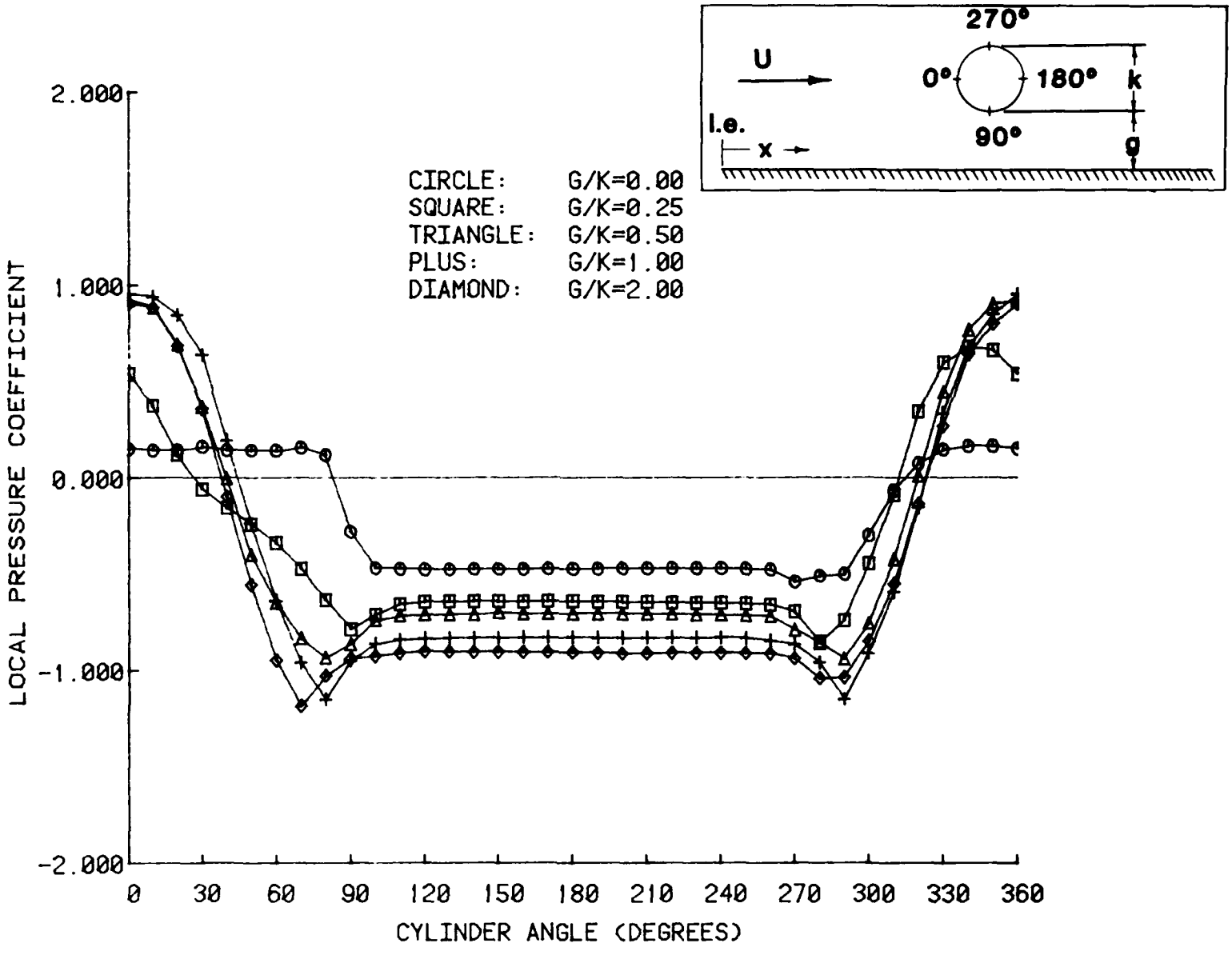

Figure A-6- Local Pressure Coefficient versus Cylinder Angle for Various Gaps ($x_k/k=48$, $R_k=3,000$)

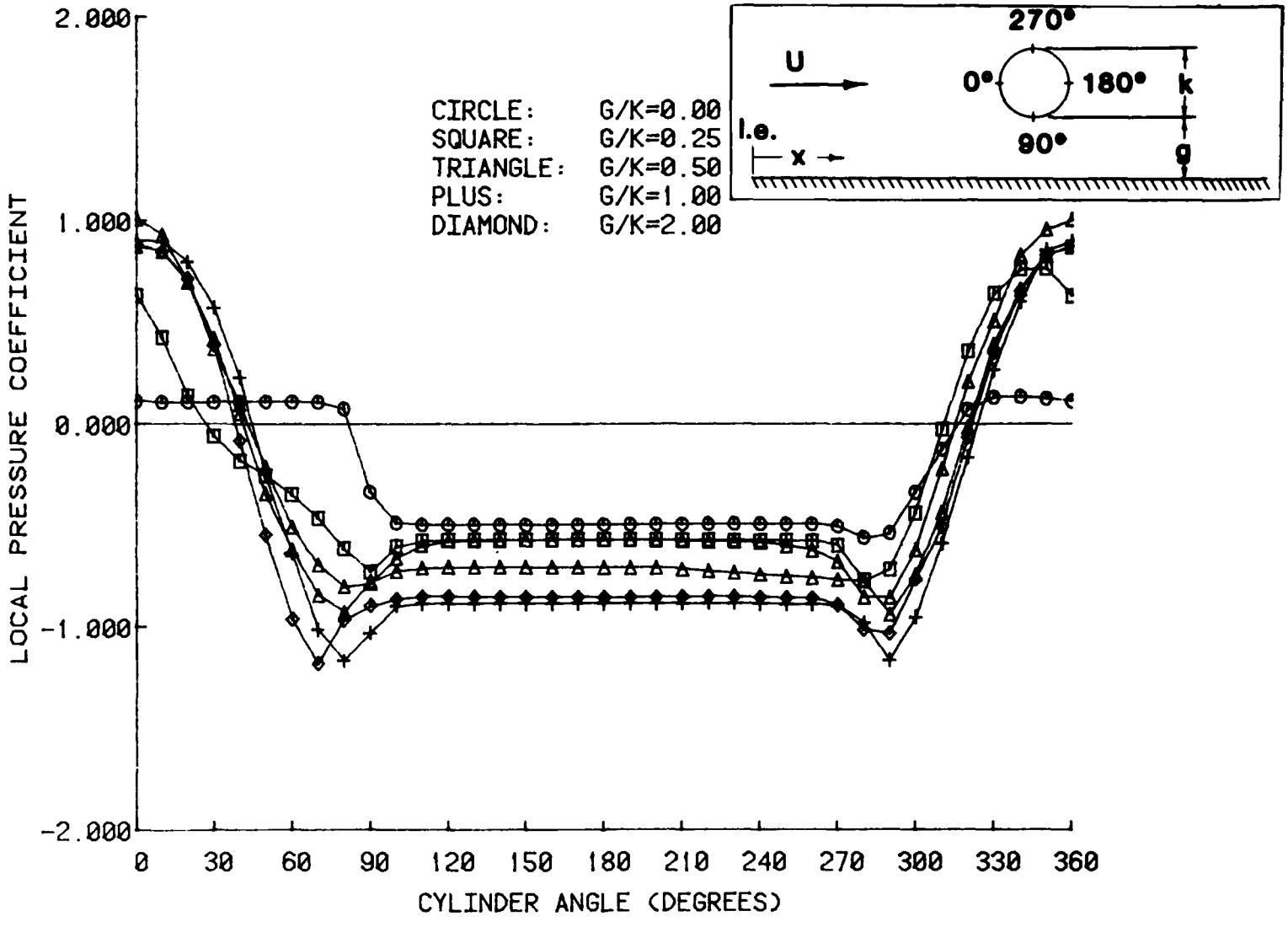

Figure A-7 - Local Pressure Coefficient versus Cylinder Angle for Various Gaps ($x_k/k=48$, $R_n=5,000$)

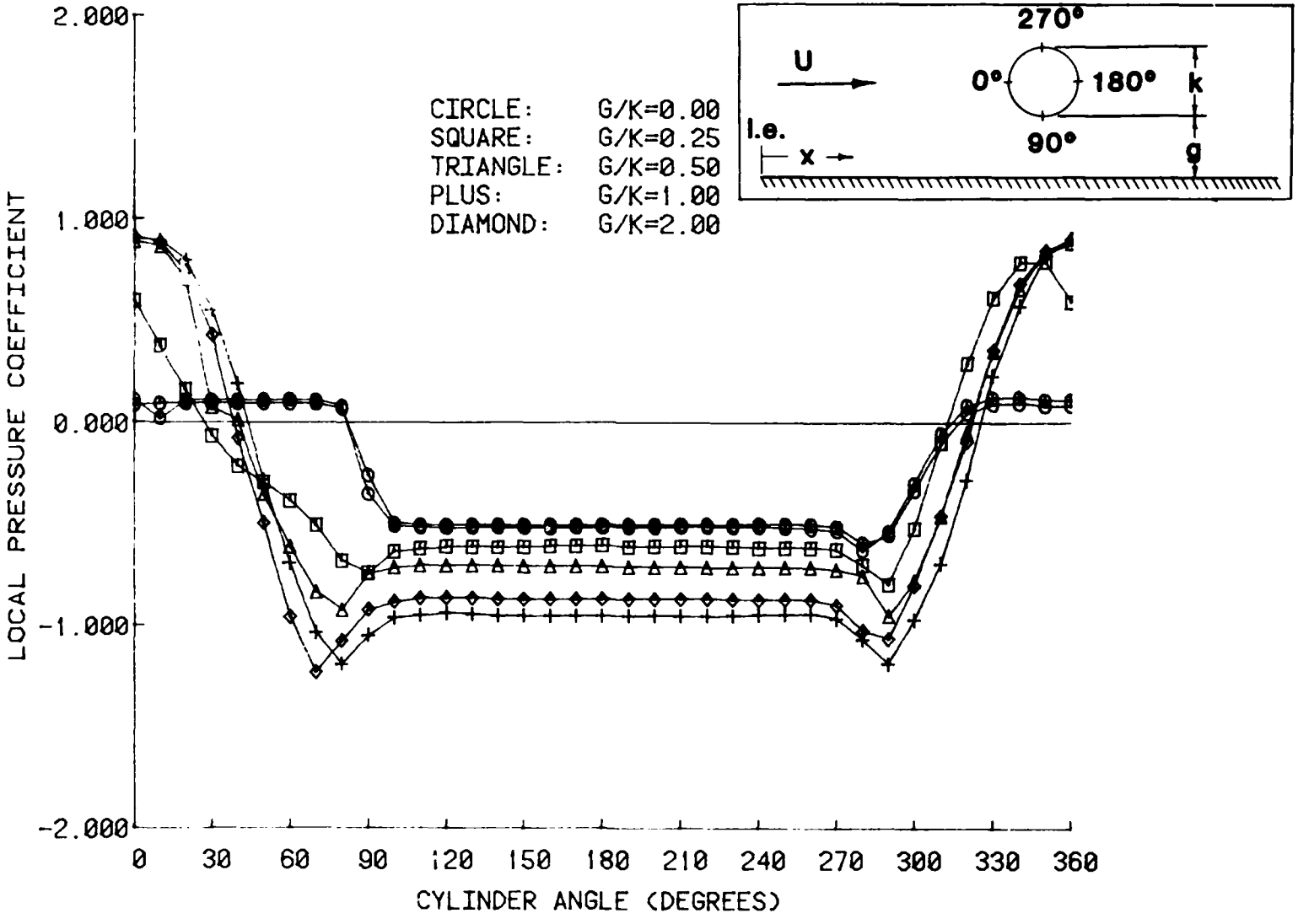

Figure A-8 - Local Pressure Coefficient versus Cylinder Angle for Various Gaps ($x_k/k=48$, $R_n=6,300$)

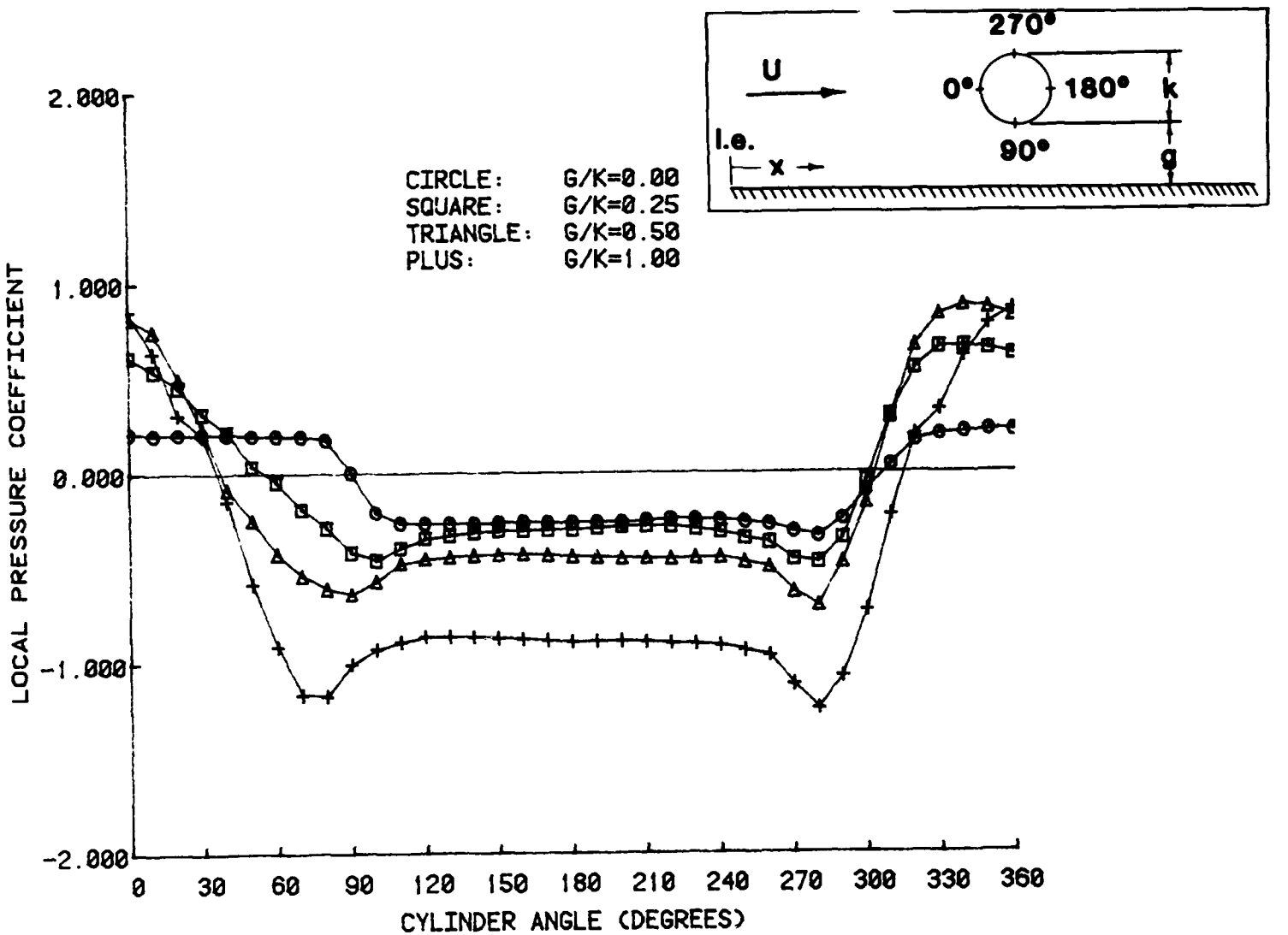

Figure A-9 - Local Pressure Coefficient versus Cylinder Angle for Various Gaps ($x_k/k=124$, $R_n=1,000$)

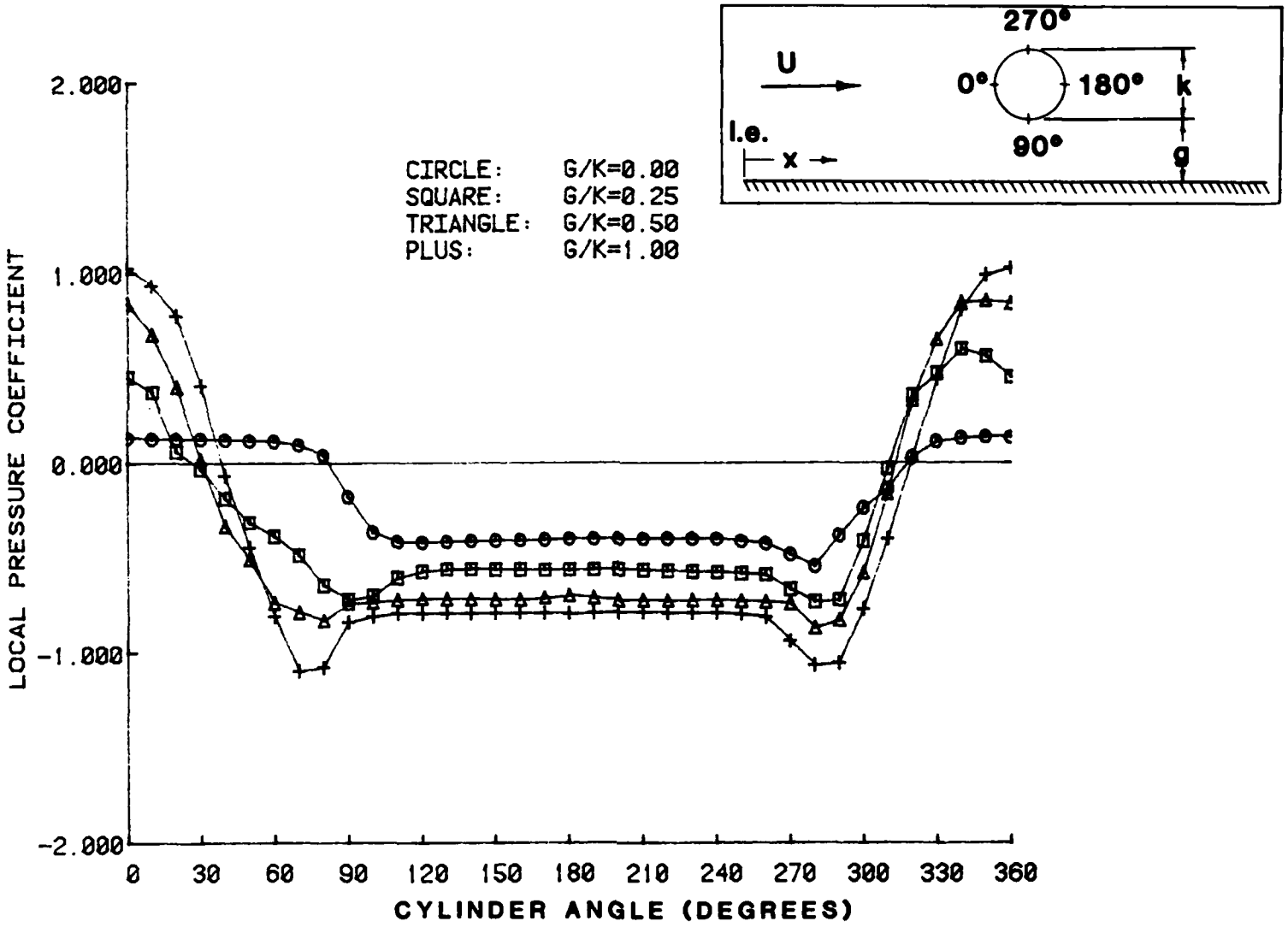

Figure A-10- Local Pressure Coefficient versus Cylinder Angle for Various Gaps ($x_k/k=124$, $R_n=3,000$)

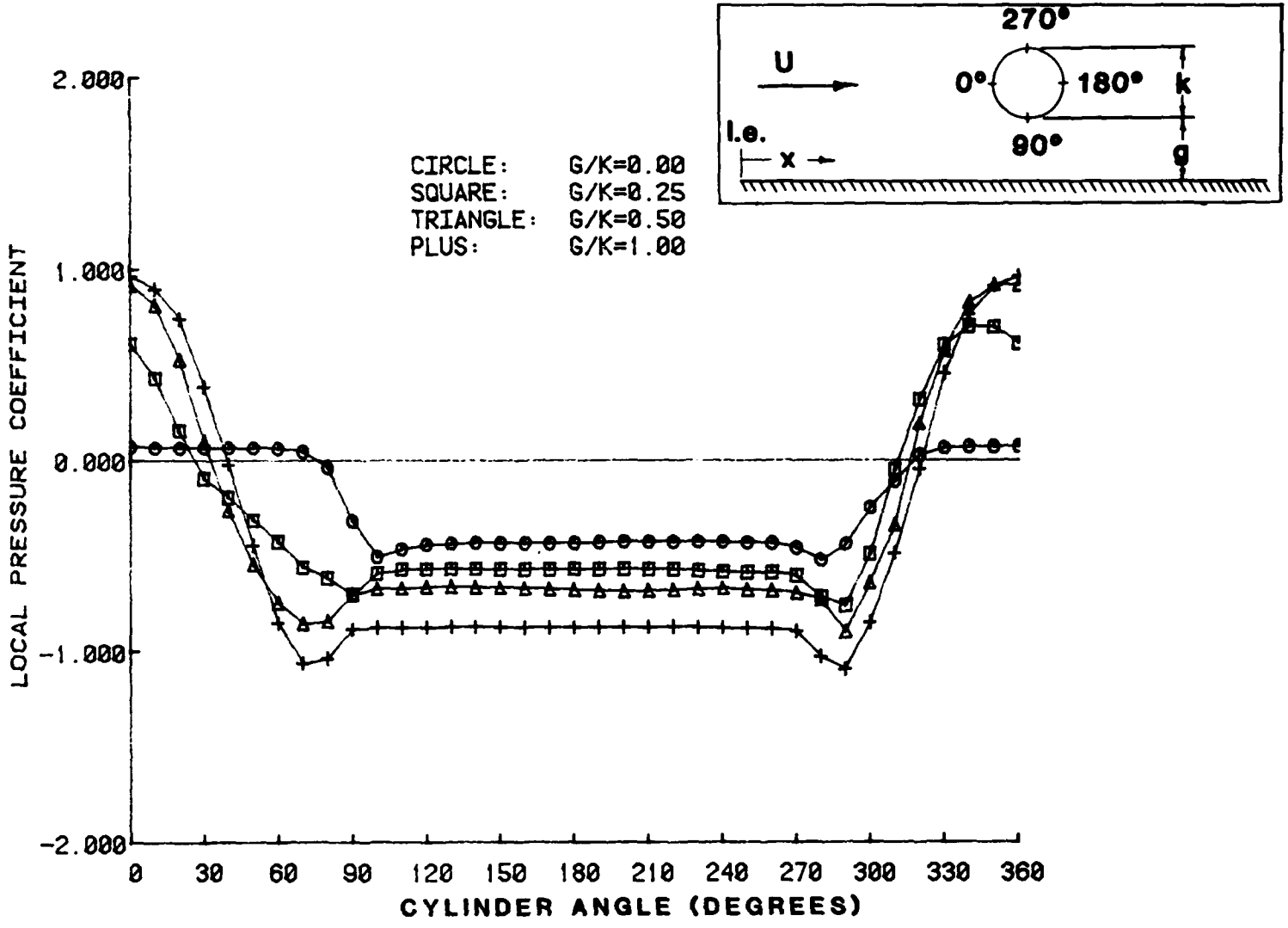

Figure A-11- Local Pressure Coefficient versus Cylinder Angle for Various Gaps (x_k/k=124, R_n=5,000)

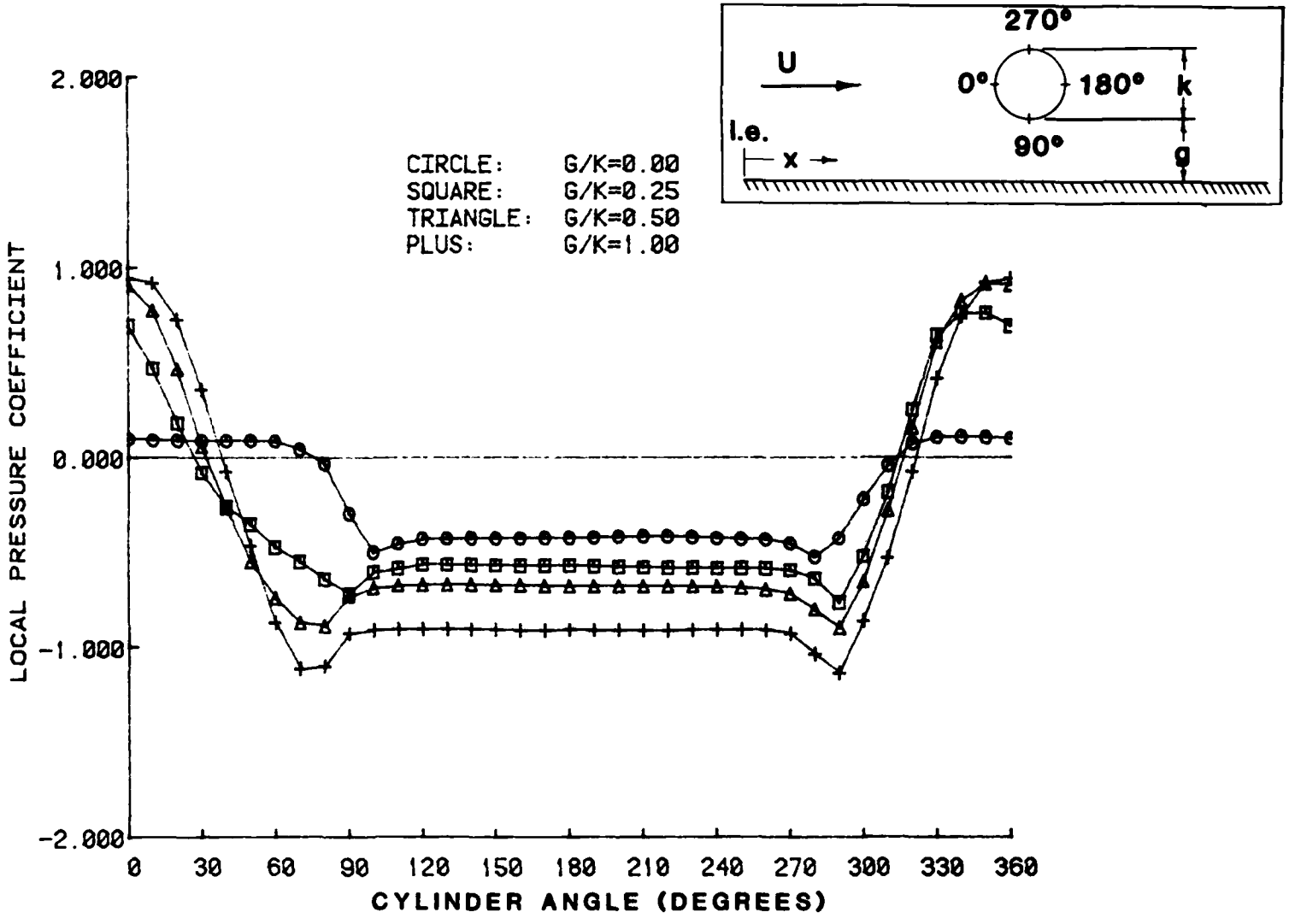

Figure A-12- Local Pressure Coefficient versus Cylinder Angle for Various Gaps ($x_k/k=124$, $R_n=6,300$)

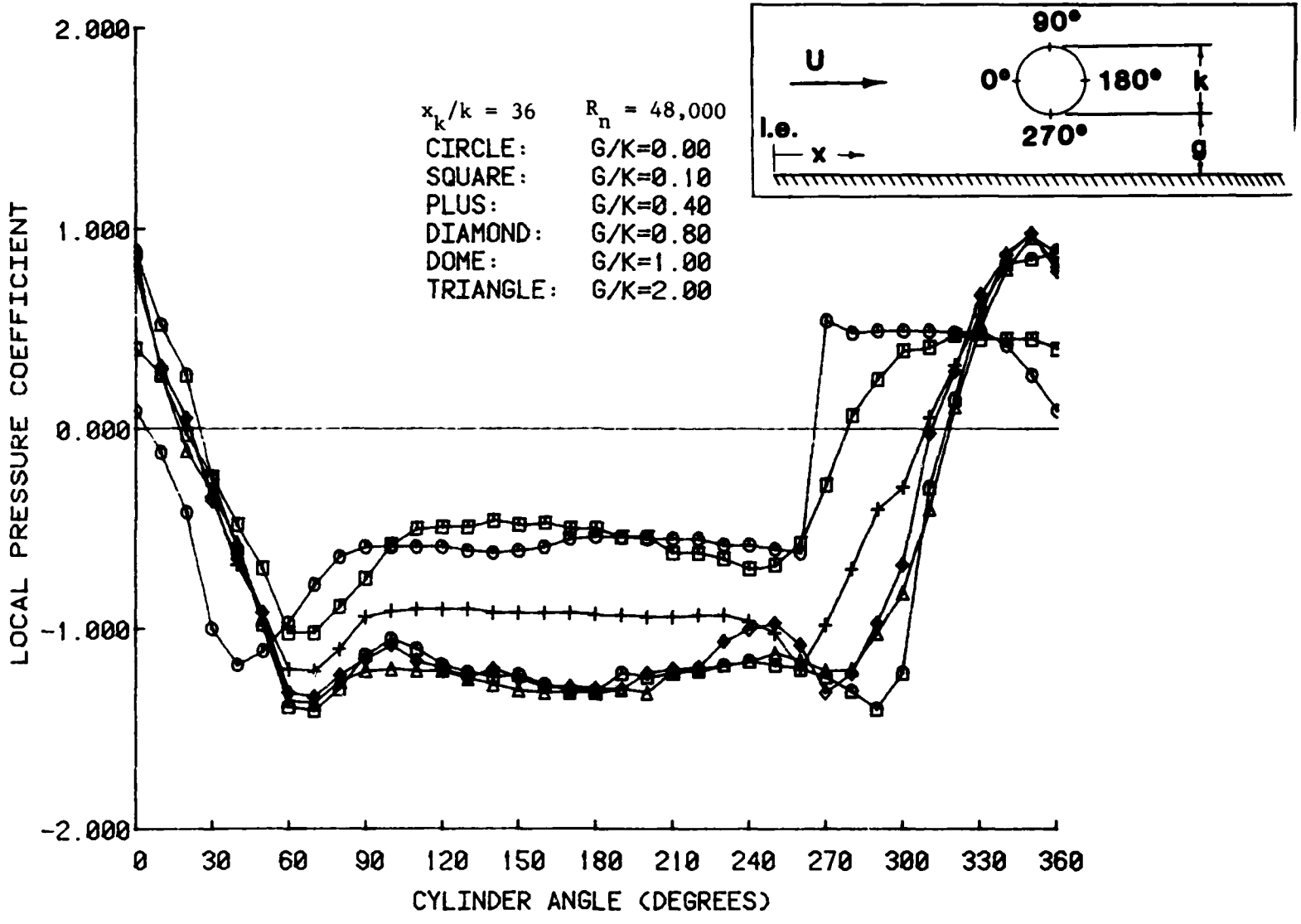

Figure A-13- Local Pressure Coefficient versus Cylinder Angle for Various Gaps (x_k/k = 36, R_n = 48,000; Bearman and Zdravkovich[7])

NOTE: ANGLE CONVENTION IS DIFFERENT FROM PREVIOUS FIGURES

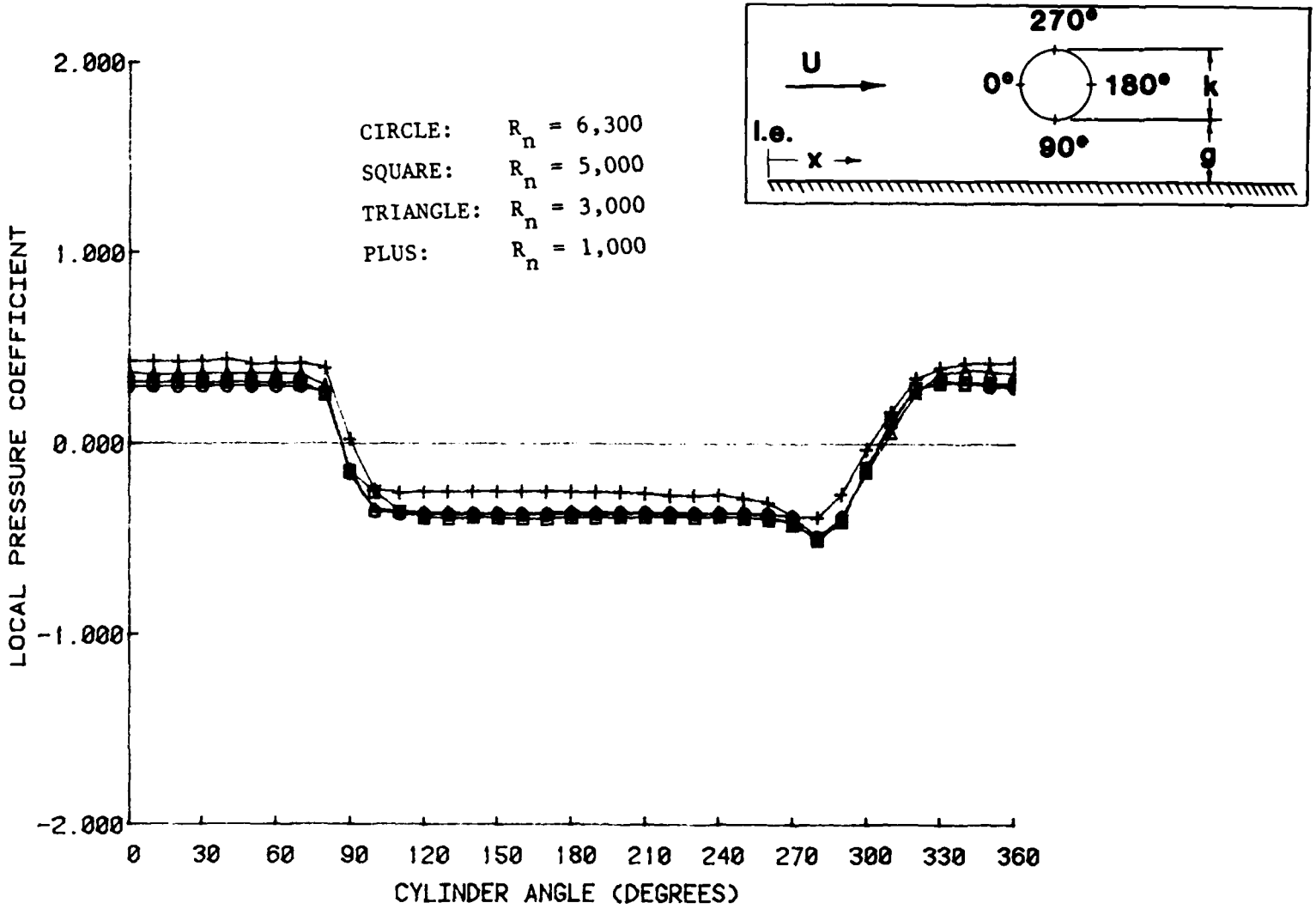

Figure A-14- Local Pressure Coefficient versus Cylinder Angle for Various Reynolds Numbers (x_k/k=24, g/k=0.00)

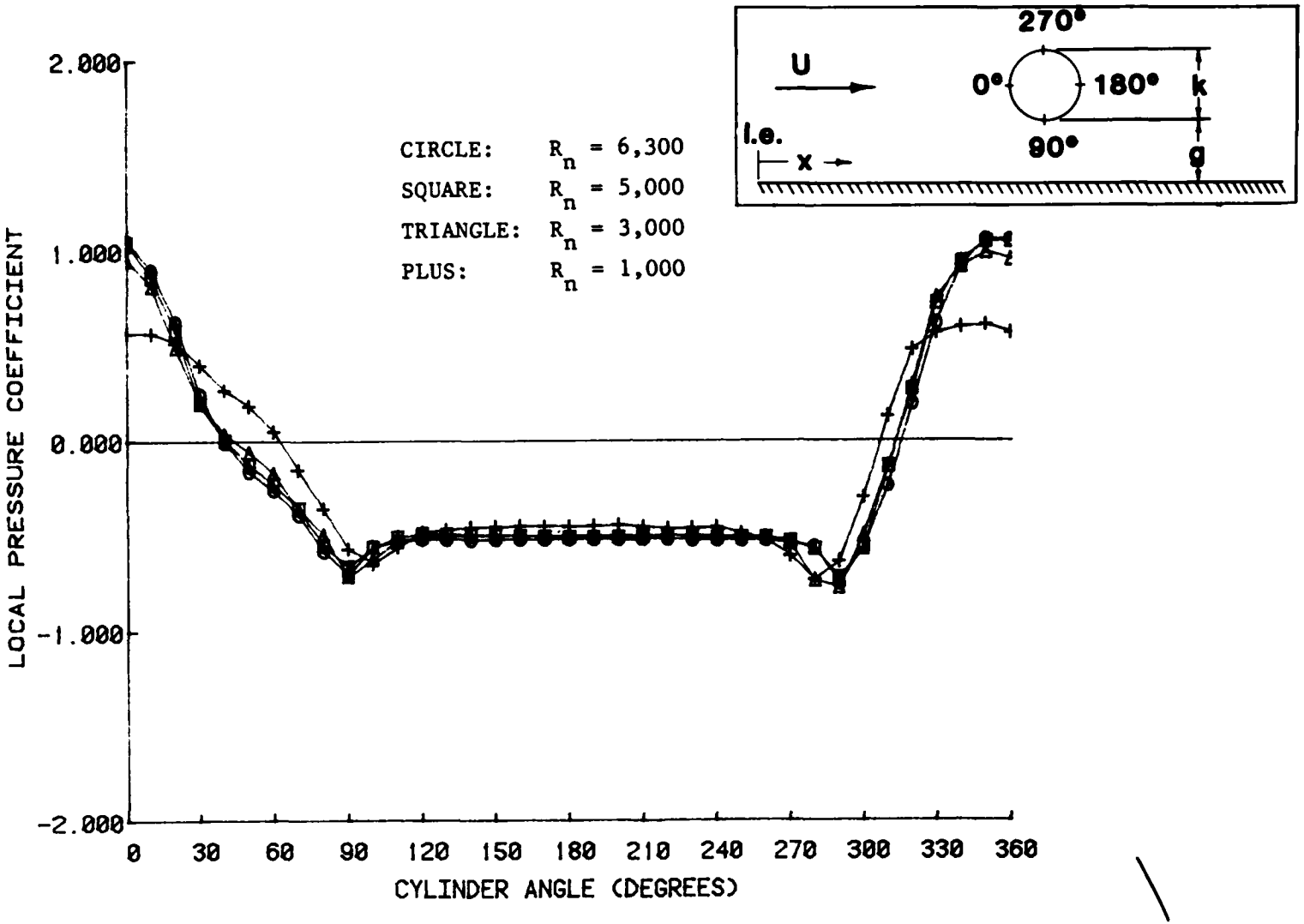

Figure A-15- Local Pressure Coefficient versus Cylinder Angle for Various Reynolds Numbers (x_k/k=24, g/k=0.25)

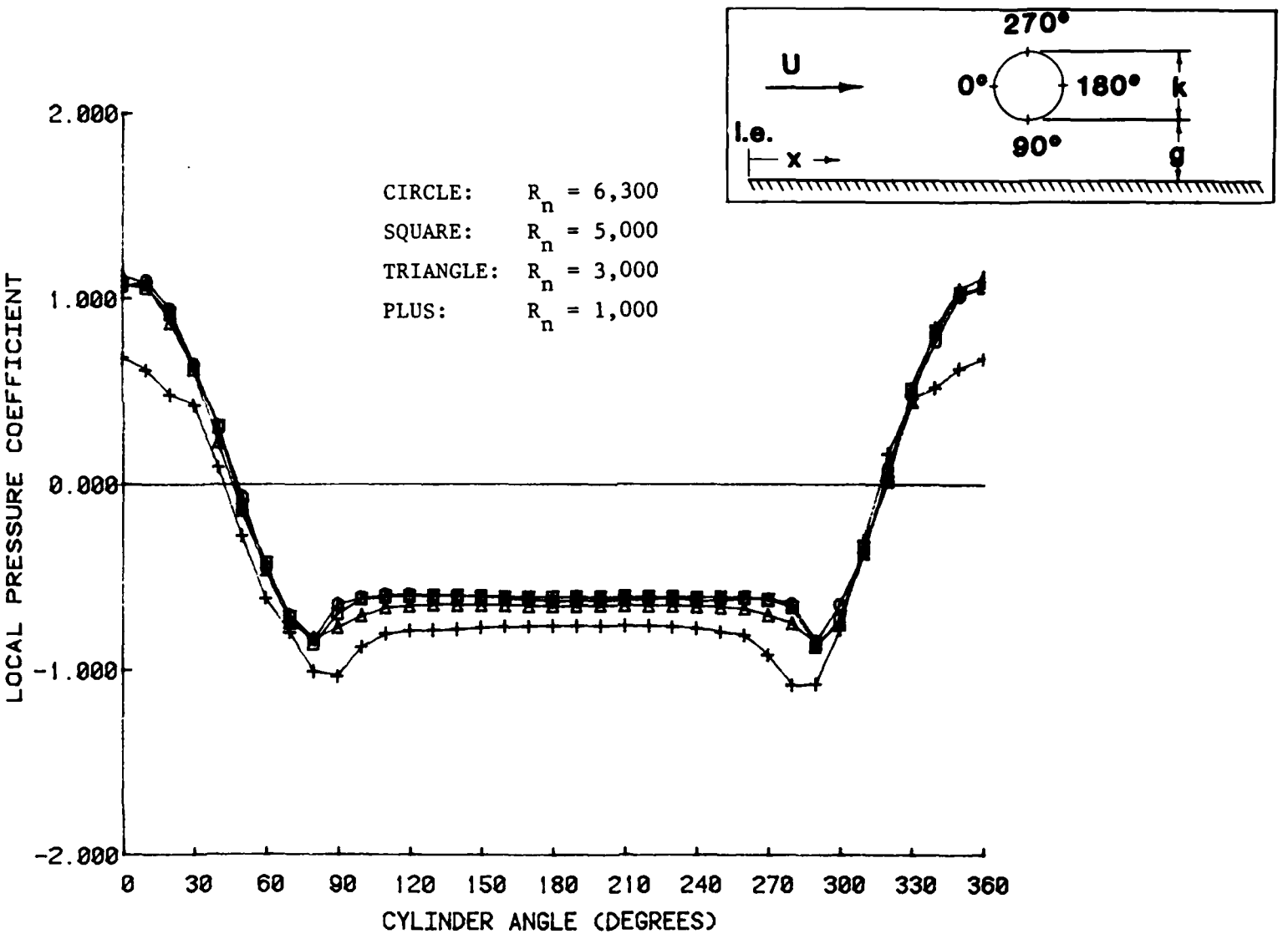

Figure A-16- Local Pressure Coefficient versus Cylinder Angle for Various Reynolds Numbers (x_k/k=24, g/k=0.50)

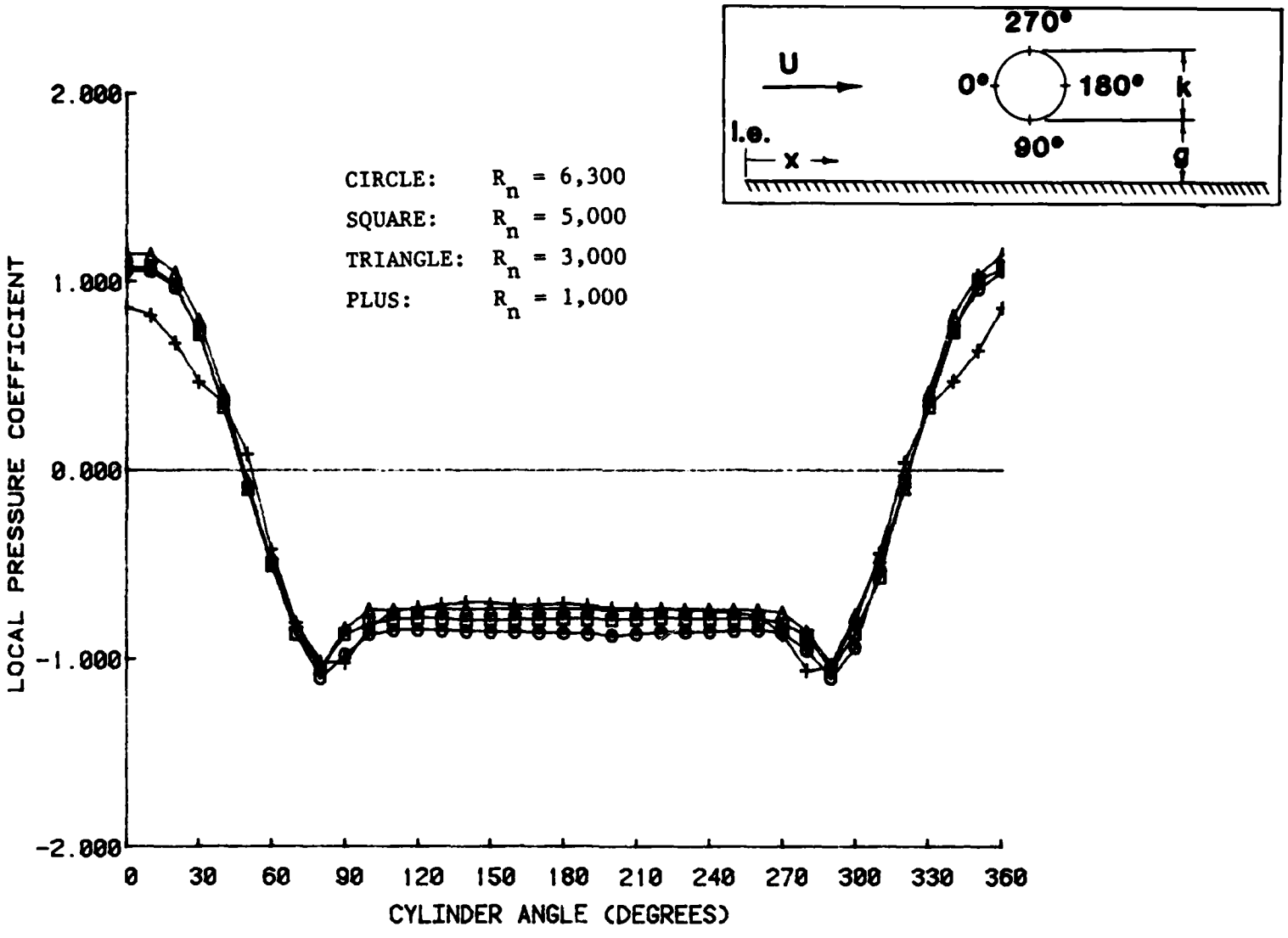

Figure A-17- Local Pressure Coefficient versus Cylinder Angle for Various Reynolds Numbers (x_k/k=24, g/k=1.00)

REFERENCES

1. Bearman P.W. and M.M. Zdravkovich, "Flow Around a Circular Cylinder Near a Plane Boundary," Journal of Fluid Mechanics, Vol. 89, pp. 33-47 (1978).

2. Roshko, A. et al., "Flow Forces on a Cylinder Near a Wall or Near Another Cylinder," Proceedings of the Second United States Conference on Wind Engineering Resources, Fort Collins, Colorado (1976).

3. Goktun, S., "The Drag and Lift Characteristics of a Cylinder Placed Near a Plane Surface," M.S. Thesis, Naval Postgraduate School (1975).

4. Wazzan, A.R., et al., "H-R_x Method for Predicting Transition," American Institute of Aeronautics and Astronautics Journal, Vol. 19, pp. 810-812, (198

5. Wazzan, A.R., et al., "Tollmien-Schlichting Waves and Tansition," Progress in Aerospace Sciences, Vol. 18, pp. 351-392 (1979).

6. Gibbings, J.C., "On Boundary-Layer Transition Wires," Aeronautical Research Council Rpt. No. 20593 (1958).

7. Preston, J.H., "The Minimum Reynolds Number for a Turbulent Boundary Layer and the Selection of a Transition Device," Journal of Fluid Mechanics, Vol 3, p. 373-384 (1957-8).

8. Tani, I. and F.R. Hama, "Some Experiments on the Effect of a Single Roughness Element on Boundary-Layer Transition," Journal of Aeronautical Sciences, Vol 20, pp. 289-290 (1953).

9. Kozlov, L.F., "Investigation of the Boundary Layer Turbulence Stimulation of Ship Models," Twelfth International Towing Tank Conference, Rome, Italy, pp. 96-99 (1969).

10. Schlichting, H., "Boundary Layer Theory," Seventh Edition, McGraw-Hull Book Company, New York, New York (1978).

11. Tani, I., and H. Sato, "Boundary-Layer Transition by Roughness Element," Journal of the Physical Society of Japan, Vol. 11, No. 12, pp. 1284-1291 (1956).

12. McCarthy, J.H. et al., "The Roles of Flow Transition, Laminar Separation and Turbulence Stimulation in the Analysis of Axisymmetric Body Drag," Eleventh Symposiuum on Naval Hydrodynamics, London, England, (1976).


4-8